

# A consistent regional dataset of dissolved oxygen in the Western Mediterranean Sea (2004-2023): CTD-O<sub>2</sub>WMED

Malek Belgacem<sup>1</sup>, Katrin Schroeder<sup>1</sup>, Marta Álvarez<sup>2</sup>, Siv K. Lauvset<sup>3</sup>, Jacopo Chiggiato<sup>1</sup>, Mireno Borghini<sup>4</sup>, Carolina Cantoni<sup>5</sup>, Tiziana Ciuffardi<sup>6</sup>, Stefania Sparnocchia<sup>5</sup>

<sup>1</sup> CNR-ISMAR, Arsenale Tesa 104, Castello 2737/F, 30122 Venice, Italy

<sup>2</sup> Instituto Español de Oceanografía, IEO-CSIC, A Coruña, Spain

<sup>3</sup> NORCE Norwegian Research Centre, Bjerknes Centre for Climate Research, Bergen, Norway

<sup>4</sup> CNR-ISMAR, Via Santa Teresa, Pozzuolo di Lerici, 19032 La Spezia, Italy

<sup>5</sup> CNR-ISMAR, Area Science Park, Basovizza, 34149 Trieste, Italy

<sup>6</sup> Department of Sustainability, St Teresa Marine Environment Research Centre, ENEA, Pozzuolo di Lerici, 19032 La Spezia, Italy

*Correspondence to:* Malek Belgacem ([malek.belgacem@ve.ismar.cnr.it](mailto:malek.belgacem@ve.ismar.cnr.it))

## Abstract.

The Mediterranean Sea is undergoing rapid change, highlighting the urgent need for high-quality, long-term datasets to investigate changes and assess impacts on its complex biogeochemical cycles. While dissolved inorganic nutrients have been well documented in the Western Mediterranean Sea (WMED) through DIN-WMED data product (Belgacem et al., 2019, 2020), reliable oxygen data have remained scarce, despite dissolved oxygen being a key driver of marine ecosystem health and central to carbon and nutrient cycling.

To fill this gap, we compiled and rigorously quality-controlled a new regional-scale dataset: CTD-O<sub>2</sub>WMED. This product comprises over 1000 unpublished high-resolution vertical profiles of sensor-based dissolved oxygen measurement collected between 2004 and 2023. The quality check process includes sensor post calibration assessment, primary quality check and a secondary quality check based on crossover analysis with established deep reference datasets, ensuring consistency and accuracy across space and time.

CTD-O<sub>2</sub>WMED provides an essential observational basis for assessing decadal oxygen variability, tracking anomalies, and improving our understanding of ventilation processes in the WMED. It also serves as a benchmark for calibrating oxygen sensor on BGC-Argo floats, and for validating regional biogeochemical models. This dataset represents a critical step toward more accurate estimation of oxygen trends in the Mediterranean Sea, an increasingly vital metric in the context of global deoxygenation and climate change.

## Data coverage

Coverage: 44° N–35° S, 6° W–14° E

Location name: western Mediterranean Sea

Date/time start: October 2004

Date/time end: April 2023

## 1 Introduction

Oxygen in the ocean is primarily produced via photosynthesis in the surface layer by phytoplankton, especially in regions of high primary productivity. The export and remineralization of organic matter from the surface, lead to oxygen consumption at depth. This can give rise to oxygen minimum zones (OMZs) or Oxygen minimum layers (OMLs), where biological respiration exceeds oxygen supply. While OMZs are prominent in certain oceanic regions, the Mediterranean Sea is generally well-oxygenated and does not exhibit OMZ but rather OML. Nevertheless, localized low oxygen events may become more frequent and intense due to ongoing climate changes (Grégoire et al. 2023).

Ocean warming and increased stratification reduce oxygen solubility and inhibit vertical mixing, thereby limiting the downward transport of oxygen-rich surface waters. These processes contribute to the expansion and intensification of low-oxygen zones, with implications for biogeochemical cycling, ecosystem function, and carbon export (Keeling et al., 2009). In deep ocean, enhanced remineralization and reduced ventilation can further exacerbate oxygen loss. Moreover, denitrification under low-oxygen conditions can alter Nitrogen to Phosphorus (N:P) ratio, influencing primary productivity and nutrient cycling.

Increased CO<sub>2</sub> levels and stratification also reshape biological communities and potentially lowering ecosystem resilience. These biogeochemical shifts affect the distribution of Oxygen and other tracers, particularly in semi-enclosed basins such as the Mediterranean Sea.

The Mediterranean Sea has experienced significant changes in recent decades, including recurrent marine heatwaves (Marullo et al., 2023; Martinez et al., 2023; Pastor and Khodayar et al., 2023), which affect oxygen distribution (Reale et al., 2022; Alvarez et al., 2023). The region's semi-enclosed nature and complex thermohaline circulation and regional differences amplify its sensitivity to climate variability (Powley et al., 2016; Testor et al. 2017; Margirier et al., 2020).

Two major events have notably altered the Mediterranean thermohaline structure. In the eastern Mediterranean (EMED), the eastern Mediterranean transient (EMT) of the mid-1990s shifted deep water formation source from colder, less saline Adriatic Deep water to warmer, more saline Aegean/Cretan Water. This new deep-water mass ventilated the Levantine basin and the Ionian Sea around 1999 and reached the Sicily channel by 2001. When the Aegean water weakened, the Adriatic deep water became dominant again between 2000 and 2010, though in subsequent years it failed to reach the deepest Ionian layers, ventilating instead the 2000-3000 m range

In the Western Mediterranean Sea (WMED), deep convection in the Gulf of Lion, has traditionally maintained the ventilation of the Western Mediterranean Deep Water (WMDW). A peak in deep water renewal occurred during the Western Mediterranean Transient (WMT) around year 2004. Since then, a decline in both the frequency and intensity of deep convection has been observed (Fourrier et al., 2020; Li and Tanhua, 2020), leading to a weakening of ventilation and intensification of the oxygen minimum at intermediate depths and affecting the uptake of atmospheric oxygen (Ulses et al., 2021).

Long-term observational programs such as the Medar/Medatlas (Fichaut et al., 2003), MED-SHIP (Schroeder et al., 2015), and MOOSE (Coppola et al., 2018) have provided valuable insights of these changes. Recent studies are using Machine learning to reconstruct higher temporal and spatial resolution Oxygen datasets by satellite and

other data sources (Liu et al., 2025). Yet, uncertainties remain about long-term impacts of deoxygenation and acidification on Mediterranean marine ecosystems (Coppola et al., 2018; Alvarez et al. 2014).

To improve understanding of regional dissolved oxygen dynamics and the impact on biogeochemical trends, this study presents a quality-controlled compilation of CTD oxygen profiles collected by the Italian National Research Council (CNR) between 2004 and 2023 in the WMED. The dataset offers reliable CTD oxygen data that can support assessments of water mass ventilation and long-term variability. This paper documents the dataset and describes the quality control procedures, including calibration assessments and corrections, to ensure the scientific reliability of oxygen measurements.

## 2 Dissolved oxygen data collection

### 2.1 The CNR data collection

The CTD-Oxygen in the **WMED** (CTD-O2WMED) dataset contains 1,382 CTD oxygen profiles collected within 25 cruises. In Figure 1, the spatial distribution of CTD profiles is depicted, highlighting the extensive coverage across the Northern Western Mediterranean (WMED) and key hydrographic transects. Measures are concentrated in the eastern part of the WMED: the subregions of the Ligurian sea, Tyrrhenian and along the Tunisia-Sicily-Sardinia area. Spanning two decades from 2004 to 2023, the dataset exhibits robust temporal coverage, particularly between 2004 and 2015 (see Fig.2a). In particular, the years 2005, 2006, 2010, and 2012 stand out with the highest number of CTD stations, coinciding with years that included monthly surveys, indicating a more frequent repeat frequency (see Fig. 2). While reasonable temporal coverage is observed between 2004 and 2015 (except for 2014), the availability of stations diminishes between 2016 and 2023.

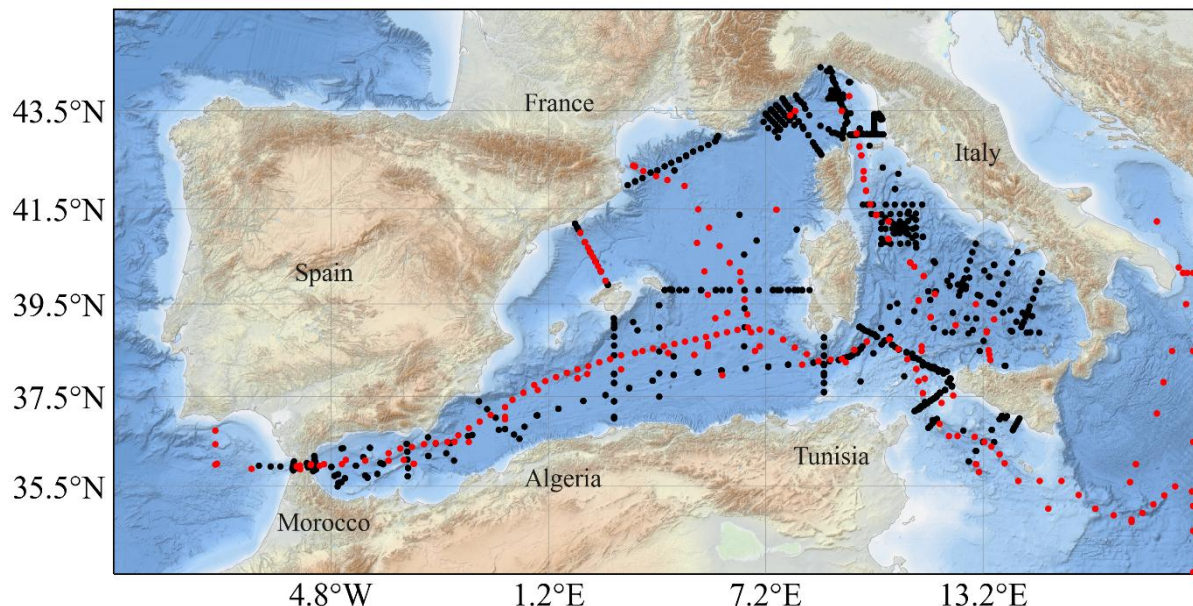


**Figure 1.** Spatial distribution of cruise stations with CTD oxygen data (black dots) in the CTDO2-WMEDv1 dataset. The red markers indicate stations (discrete measurements) from the reference.

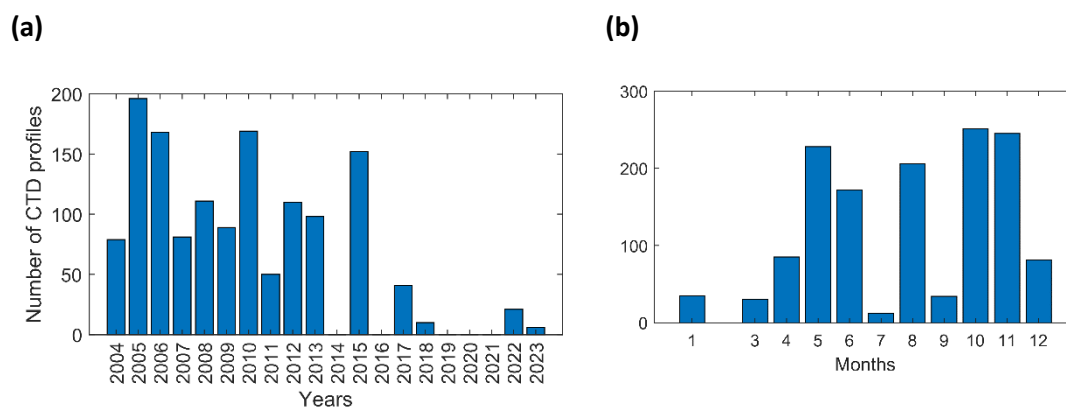


**Figure 2.** Temporal distribution of CTD oxygen profiles: A. annual distribution and B. monthly distribution.

- Assessment of sensor calibration

Dissolved oxygen has been measured using Sea-Bird (SBE43) oxygen sensor mounted on the CTD rosette, and by Winkler titration of discrete samples collected in Niskin bottles at various depths. These samples were analyzed onboard by different research team. In this dataset, we only evaluate the CTD sensor oxygen data, which were post-calibrated against Winkler measurements as summarized in Figure 3. Note that discrete Winkler data are not included in the final product.

The cruises listed in Table 1 were calibrated using Winkler titrations, following standard procedures (Grasshoff et al. 1983; Langdon, 2010). Discrete samples were used to calibrate the CTD sensor, correcting for sensor drift, in line with the approaches of Janzen et al. (2007) and Uchida et al. (2010). Calibration methods followed the application note SBE 43 DO Sensor calibration and data correction (NO.64-2 from Sea-Bird Electronics, [www.seabird.com](http://www.seabird.com)).

Following Uchida et al. (2010), we assess the residuals between Winkler (O<sub>2</sub> bottle) sensor (O<sub>2</sub> sensor) after calibration, or calibration limitations. Sensor data were matched to discrete samples based on pressure. For cruises where more than one SBE43 sensor was deployed, the sensor with the smallest residuals relative to the Winkler samples was selected for this assessment.

Figure 3(a) shows of the residuals (O<sub>2</sub> bottle–O<sub>2</sub> sensor) plotted against pressure, with cruises color-coded by start date. residuals are generally smaller below 800 db, though systematic differences up to  $\pm 15 \mu\text{mol/kg}$  are observed. Figure 3(b) presents the residual distribution for each cruise using boxplots. High variability (standard deviation of the mean residual  $> 7 \mu\text{mol/kg}$ ) is observed for cruises such as 48UR20080905, 48UR20050412, 48QL20171023 and 48UR20041006.

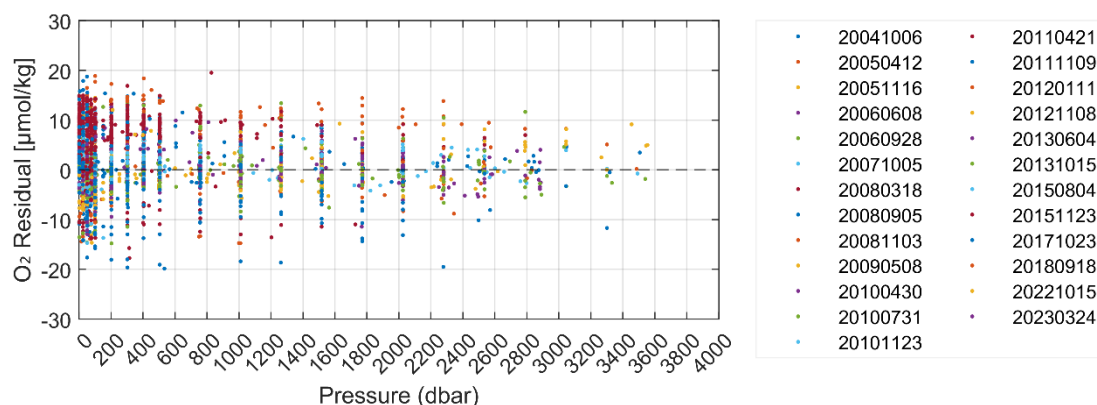
In 48UR20080905, only five Winkler samples limiting calibration quality. For 48UR20050412, which had two legs samples from one leg were used to calibrate the entire cruise. Some cruises (e.g., 48UR20060608) show pressure-dependent residuals, indicating issues with pressure compensation during calibration.

Figure 3(c) summarized cruise-level agreement using the mean residual and the percentage of values within  $\pm 2 \mu\text{mol/kg}$ . According to Uchida et al., (2010), residuals should remain within this threshold after proper calibration. Cruises were color-coded as follows: Green indicates cruises where  $\geq 40\%$  of residuals within  $\pm 2 \mu\text{mol/kg}$

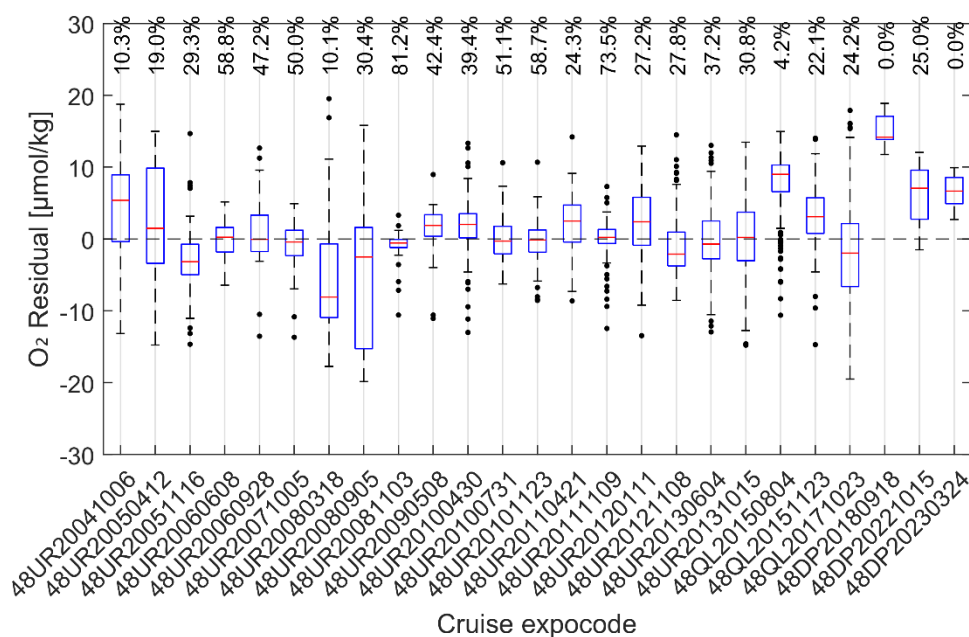
127 (considered good agreement); Blue represent moderate or uncertain agreement (19 to <40% of mean residual  
 128 within  $\pm 2 \mu\text{mol/kg}$ ); Grey denotes cruises with systematic bias (<19% of mean residual  $>2 \mu\text{mol/kg}$ ).

129 Eight cruises show good agreement, eleven are moderate, and the rest display systematic positive or negative  
 130 biases. These may reflect sensor calibration issues, bottle handling problems, or sensor drift. This analysis helps  
 131 flag suspect data for correction or further review. We do not discuss each cruise individually, as the purpose here  
 132 is to assess the outcome of the calibration process.

(a)



(b)



(c)

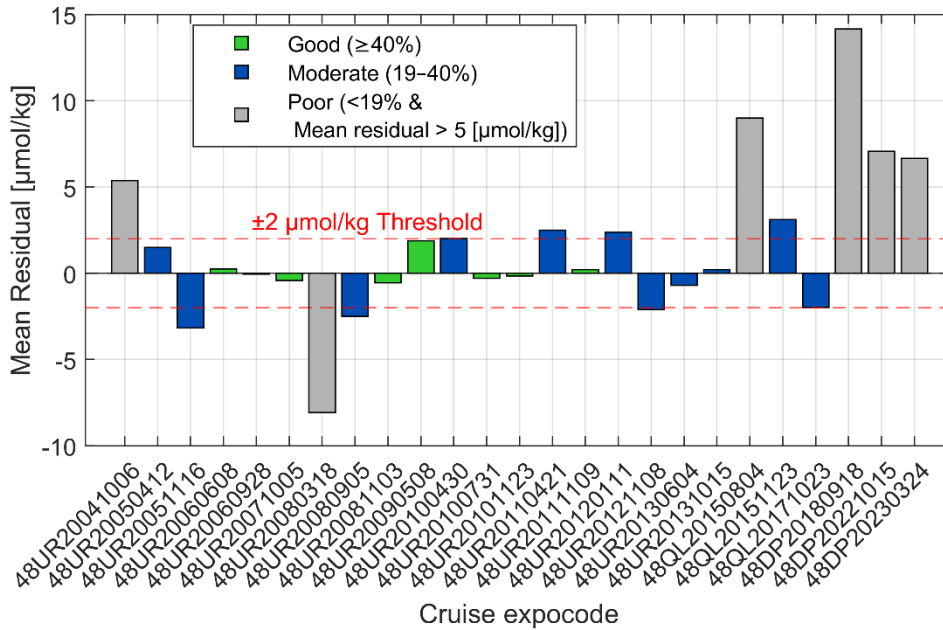


**Figure 3.** Residuals between CTD oxygen data from SBE43 (sensor) and Winkler oxygen data (O2 bottle) for (a) all dataset against pressure color coded with each cruise starting date; (b) boxplot distribution with % of residuals within  $\pm 2 \mu\text{mol/kg}$  and, (c) assessment of the mean residual of each expocode/cruise.

**Table 1.** Cruise summary table listed with number of stations. Refer to Belgacem et al. (2020) and Ribotti et al. (2022) for cruise metadata.

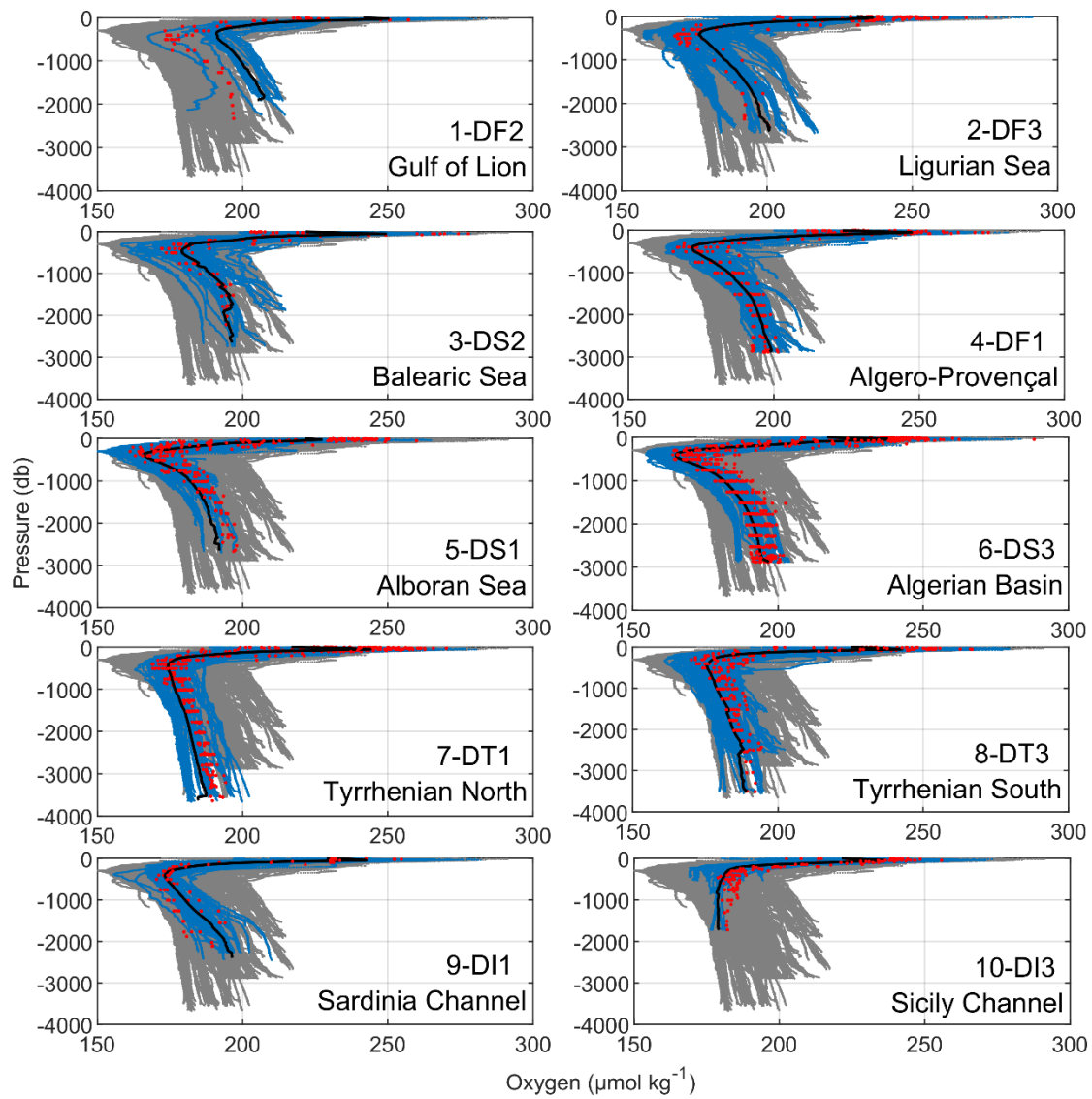
Cruise ID	Cruise	Expocode	Research vessel (RV)	Date Start/End	Nb CTD profile
2	MEDGOOS9	48UR20041006	Urania	6 - 25 OCT 2004	82
3	MEDOCC05/ MFSTEP2	48UR20050412	Urania	24 APR - 16 MAY 2005	160
5	MEDGOOS11	48UR20051116	Urania	16 NOV - 3 DEC 2005	36
6	MEDOCC06	48UR20060608	Urania	8 JUN - 3 JUL 2006	127
8	MEDGOOS13/MEDBIO06	48UR20060928	Urania	28 SEP - 8 NOV 2006	41
9	MEDOCC07	48UR20071005	Urania	5 - 29 OCT 2007	81
10	SESAMEIt4 KM3 or SESAME_KM3	48UR20080318	Urania	18 MAR - 7 APR 2008	27
11	SESAMEIT5 (Sesame KM3 September 2008)	48UR20080905	Urania	5 - 16 SEP 2008	24
12	MEDCO08	48UR20081103	Urania	3 - 24 NOV 2008	60
13	TYRRMOUNTS	48UR20090508	Urania	8 MAY - 3 JUN 2009	86
14	BIOFUN010	48UR20100430	Urania	30 APR - 17 MAY 2010	29
15	VENUS1	48UR20100731	Urania	31 JUL - 25 AUG 2010	116
16	BONSIC2010	48UR20101123	Urania	23 NOV - 9 DEC 2010	24
17	EUROFLEET11	48UR20110421	Urania	21 APR - 8 MAY 2011	31
18	BONIFACIO2011	48UR20111109	Urania	9 - 23 NOV 2011	18
20	ICHNUSSA12	48UR20120111	Urania	11 - 27 JAN 2012	35
21	EUROFLEET2012	48UR20121108	Urania	8 - 26 NOV 2012	75
211	VENUS 2	48UR20130604	Urania	4 - 25 JUN 2013	59
22	ICHNUSSA13	48UR20131015	Urania	15 - 29 OCT 2013	40
222	ICHNUSSA15	48QL20151123	Minerva Uno	23 NOV - 14 DEC 2015	62
23	OCEANCERTAIN15	48QL20150804	Minerva Uno	4 - 18 AUG 2015	90
24	ICHNUSSA17/INFRAOC E17	48QL20171023	Minerva Uno	23 OCT- 28 NOV 2017	41
25	ICHNUSSA/JERICO18	48DP20180918	DallaPorta	18-25 SEP 2018	10
27	JERICO-II-2022	48DP20221015	DallaPorta	15- 25 OCT 2022	21
28	JERICO-III-EurogoShip-2023	48DP20230324	DallaPorta	24 MAR - 09 APR 2023	6



The vertical distribution of dissolved oxygen in the WMED reflects the interplay between air-sea gas exchange, biological activity, and regional circulation processes. In the surface waters, oxygen concentrations remain close to atmospheric saturation due to gas exchange and photosynthetic production by phytoplankton. As organic matter sinks and is re-mineralized in subsurface waters, oxygen is consumed, giving rise to vertical gradients. However, unlike any other ocean basins where pronounced Oxygen minimum zone develops, the WMED remain relatively well-oxygenated owing the periodic deep convection events in the Gulf of Lion (DF2) which generate the WMDW. This dense, oxygen -rich water mass ventilates deep layers across subregions such as the Algerian (DS3, DF1), Ligurian (DF3) and Gulf of lion (DF2) which are known to be among the most ventilated areas (Schneider et al., 2014).

To provide a comprehensive view of this oxygen distribution, Fig. 4a presents the vertical CTD oxygen profiles versus pressure across ten WMED subregions defined in Fig.4b, alongside data from reference cruises (Table 2). The blue shading highlights the oxygen concentration range within each subregion, revealing clear spatial differences across depth layers. one recurring feature is the intermediate depth oxygen minimum layer (OML), typically found between 300 and 600 db. This layer corresponds to the core of the LIW, which is warmer, saltier, and consistently lower in oxygen compared to surrounding water (Tanhua et al., 2013; Coppola et al., 2018; Mavropoulou et al., 2020). The depth, thickness, and intensity of the OML vary regionally and interannually, influenced by remineralization rates, nutrient availability, mixing intensity and regional circulation (Coppola et al., 2018). In the Tyrrhenian subregion, the OML is followed by increasing Oxygen concentrations at depth, suggesting downward diffusion of more oxygenated water. In contrast, the lowest oxygen concentrations in the WMED are observed in the Sicily channel and Tyrrhenian Sea, where the LIW is prominent and deep ventilation is weak. Meanwhile on the Alboran and Balearic seas exhibit relatively well(oxygenated profiles through the water column, a result of both the influence of the WMDW and enhanced vertical fluxes driven by mesoscale and sub-mesoscale processes that transport oxygen-rich surface water downward (Middleton et al., 2025).

(a)



(b)

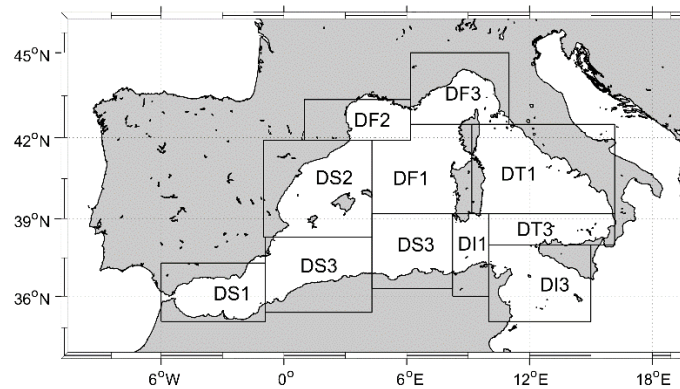


**Figure 4.** (a) Overview of CTD oxygen distribution versus pressure for the WMED in grey, from the original dataset after the initial quality control (1st QC). The blue represents the vertical distribution within each subregion (refer to Table S1). The black lines denote the mean profile of each subregion over the entire period. The red dots denote the reference data. (b) Geographical map indicating the geographical limits from MEDAR/Medatlas subregions (defined in Table S1, adapted from Manca et al. (2004)).



### 3 Quality control methods

#### 3.1 Primary quality control of CTD-O2 data

Each cruise was converted to standard units. The GSW toolbox was used to calculate conservative temperature (CT), absolute salinity (SA), and potential density. Dissolved oxygen was converted from milliliters per liter (ml L<sup>-1</sup>) to micromoles per kilogram ( $\mu\text{mol kg}^{-1}$ ) using potential density and the conversion factor 44.66 to ensure uniformity. Then each cruise went through a rigorous scan for outliers. each parameter was assigned a data quality flag. Initially set to 2 for acceptable values, flag 3 for questionable values and to 9 for data following WOCE.

However, the cruises did not necessarily have all parameters analyzed to the highest standards, and insufficient metadata. There often are insufficient deep stations to compare data with reference data. The primary quality control (1<sup>st</sup> QC) procedure involved the identification of outlier profiles and/ or data points in each cruise. Outliers were flagged, indicating the quality of each value (refer to Table 3 in Belgacem et al., 2020). Flagging was specific to the precision of each parameter for each cruise. Property-property plots were examined for each region, and values identified as outliers in more scatter plots were flagged as questionable. Approximately 0.2% of CTD O2 data were considered outliers and flagged as 3. The 1<sup>st</sup> QC can be subjective, as it relies on the expertise of the individual inspecting the data.

To assess the internal consistency and precision of the CTD oxygen data across cruises, we computed Median and median absolute deviation (MAD) of deep oxygen concentrations (>800 dbar, as summarized in Fig.6 and Table S3, in supplementary) to sidestep any variability associated with atmospheric forcing or mesoscale variability and residual outliers.

Figure 5 (a) highlights the spatial variability in deep-water oxygen concentrations across the WMED. A distinct east-west gradient is evident, with lower oxygen levels (blue tones) characterizing the eastern subregions, including the Tyrrhenian Sea, Sardinia channel, and Sicily channel; in contrast, higher oxygen concentration (green to yellow) is observed in the westernmost regions, reflecting enhanced ventilation associated with deep convection processes in the Gulf of Lion. MAD was used as a proxy for precision, while comparisons of cruise-level medians with regional medians served to identify potential biases or systematic offsets.

Overall, MAD values ranges from 0.1 to 7.5  $\mu\text{mol/kg}$ . in well-sampled subregions ( $\geq 5$  cruises), high MAD or anomalous medians were used to recognize potentially problematic cruise.

In the Ligurian Sea (DF3), among five cruises, cruise #3 and #21 exhibited the highest MAD. While cruise 2, had a median consistent with other cruises, cruise #3 was  $\sim 10 \mu\text{mol/kg}$  lower, and cruise #6 was  $\sim 6 \mu\text{mol/kg}$  higher, despite a low MAD. This discrepancy suggests potential bias or calibration issues, especially for cruise #6.

In the Balearic Sea (DS2), six cruises sampled the deep waters. All but cruises #3 and #6, showed low MAD. These two cruises had MADs of 5.4 and 6.9  $\mu\text{mol/kg}$ , respectively, raising concerns about their precision.

In the Algéro-Provençal region (DF1), ten cruises sampled this subregion. Cruise #24 has the highest MAD (7.5  $\mu\text{mol/kg}$ ) and the highest median but was also based on only two profiles, likely explaining the high uncertainty. cruise #3 again showed an anomalously high median (197.6  $\mu\text{mol/kg}$ ), and cruise #6 has an elevated MAD of 4.2  $\mu\text{mol/kg}$ .

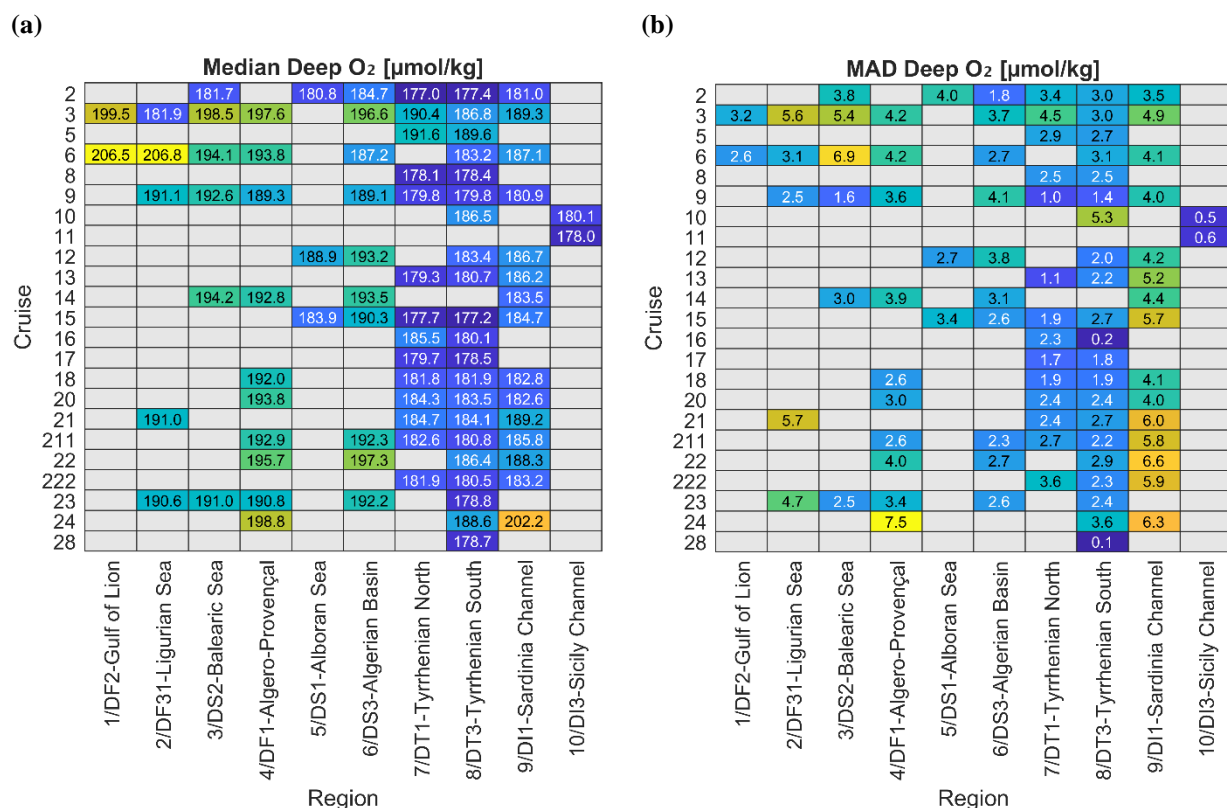
213 In the Algerian basin (DS3), ten cruises showed generally good agreement (MAD between 1.8 and 4.1  $\mu\text{mol/kg}$ ).  
 214 however, cruise #22 (2013) had an elevated oxygen value, potentially capturing a real increase in deep oxygen. In  
 215 contrast, cruise #3 (2005), showed a regionally anomalous median, suggesting possible quality issues.

216 In the Tyrrhenian North region (DT1), with 14 cruises, this region has MADs from 1 to 4.5  $\mu\text{mol/kg}$ . Cruises #3  
 217 and #222 displayed larger MADs and only cruise #3 had high median, while cruise #2 recorded the lowest deep  
 218 oxygen concentrations.

219 In the Tyrrhenian South region (DT3), the most frequently sampled region (20 cruises). MADs ranged from 0.1  
 220 and 5.3  $\mu\text{mol/kg}$ . elevated MADs were observed in cruise #2, #3, #5, #6, #10, and #24, suggesting noise.

221 In Sardinia Channel (DI1), fifteen cruises showed relatively consistent medians, but MAD values were generally  
 222 higher (3.5 to 6.5  $\mu\text{mol/kg}$ ). Recent cruises, particularly cruise #24, showed the highest median (202.2  $\pm$  6.3  
 223  $\mu\text{mol/kg}$ ), significantly higher than earlier cruises, possibly indicating calibration issues.

224 Following the approach adapted from Olsen et al. (2016), large MADs combined with anomalous medians and  
 225 limited spatial coverage (i.e., subregions) point to low internal precision and potential systematic error. Cruise #3  
 226 (multiple subregions) is consistently showing high MAD or biased medians. Cruise #6 (DF3, DS2, DT3) has an  
 227 unusually high median in DF3 and high MAD in DS2 and DT3. Cruise #24 (DS3, DT1) is showing an elevated  
 228 deep oxygen and large MAD, save for Cruise #22. Cruise #2 (DT1, DT3) show low median and high MAD,  
 229 possibly indicating systematic error, same for cruise #5.



230 **Figure 5.** Median and MAD of deep CTD oxygen concentrations (>800 dbar). Heatmaps showing (a) the median  
 231 and (b) the median absolute deviation (MAD) of CTD dissolved oxygen concentrations at pressure >800 dbar,  
 232 organized by cruise (rows) and geographic subregion (columns), Grey color indicate no data. These metrics

support the intercomparison of deep oxygen distribution and data quality across the CTDO2-WMED dataset, (Table S3).

### 3.2 Secondary quality control: crossover analysis

The secondary quality control (2<sup>nd</sup> QC) method involves comparing the CNR cruises with reference cruises. The reference data are assumed to be accurate, and stable, particularly in deep water; however, this assumption may not always be effective, for more recent cruises due to the region's strong spatial gradients and potential long-term changes in dissolved oxygen concentrations. In global data synthesis efforts such as GLODAP and CARINA, a 1% agreement threshold has been widely used in crossover analysis to detect potential biases and ensure consistency across cruises. However, this could don't be valid for the case of the Mediterranean Sea. These changes may affect the entire Basin in long-term, particularly the intermediate and deep water. Here, we check the consistency of the reference dataset, test and identify accuracy thresholds and identify the least variable depth range on which to apply the Xover analysis.

- *Reference data:*

The previously described CNR CTDO<sub>2</sub> profile data collection is compared to deep water observation from the same area. A total of seven cruises have been identified (Table 2, Figure 6) with documented high-quality dataset during which discrete oxygen measurements were collected in the Mediterranean Sea through international projects. Defined as "reference cruise," they adhere to the recommendations of the World Ocean Circulation Experiment (WOCE) and the Global Ocean Ship-Based Hydrographic Investigations Program (GO-SHIP) protocols (Langdon 2010). Among these, cruises 06MT20011018 and 06MT20110405 are significant surveys, contributing to the GLODAPv2 dataset (Olsen et al., 2016). During these cruises, quality control procedures were applied, and minimal corrections to oxygen measurements were made, ensuring excellent data quality. Additional information regarding these cruises can be found in the work of Tanhua et al. (2013a) and Hainbucher (2012). For further details, one can refer to the adjustment table available at <https://glodap.info/> (last access: August 2024) and the work by Olsen et al. (2020).

Similarly cruises 48UR20070528 (TRANSMED II), 29AH20140426 (HOTMIX) and 06M220180302 (MSM72) which are related to CARIMED (CARbon, tracer, and ancillary data In the MEDsea) that aims to be an internally consistent database containing inorganic carbon data (Álvarez et al., in preparation); which means that this cruise underwent rigorous quality control processes. The TALPpro cruises conducted in 2016 (Tanhua, 2019a, 2019b; Jullion, 2016) and in 2022 (Schroeder, 2022) are associated with the MedSHIP program, which follows the guidelines established by the international GO-SHIP initiative. This program is dedicated to high-quality data collection and analysis to evaluate the impacts of climate on marine environments (Schroeder et al., 2015, 2024). Following the standards and charts of these programs, the quality of measurements obtained during these cruises has been ensured, demonstrating both precision and reliability, and thus used as reference cruises in the 2<sup>nd</sup> QC. To sum-up, we are using these bottle oxygen reference from seven cruises to check and evaluate the CTD-O2 sensor-based dataset.

**Table 2.** Overview of reference dataset utilized in the 2<sup>nd</sup> QC process with their Expocode and Identification number (ID). The data spans from 2001 to 2022.

ID	Common name	EXPCODE	Date starts and end	Stations	Source	Chief scientist(s)
6	<i>M51/2</i>	06MT20011018	18 Oct–11 Nov 2001	6	GLODAPv2	Wolfgang Roether
<i>TRANSMED_LEG</i>						
22	<i>II</i>	48UR20070528	28 May–12 Jun 2007	4	CARIMED	Maurizo Azzaro
64	<i>M84/3</i>	06MT20110405	5–28 Apr 2011	20	GLODAPv2	Toste Tanhua
17	<i>HOTMIX</i>	29AH20140426	26 Apr–31 May 2014	18	CARIMED	Javier Aristegui
27	<i>TAIPro-2016</i>	29AJ20160818	18–28 Aug 2016	42	MedSHIP programme	Loïc Jullion, Katrin Schroeder
72	<i>MSM72</i>	06M220180302	2 Mar–3 Apr 2018	130	Go-SHIP	Jens Karstens
28	<i>TAIPro-2022</i>	11BG20220517	17–26 May 2022	24	MedSHIP programme	Katrin Schroeder

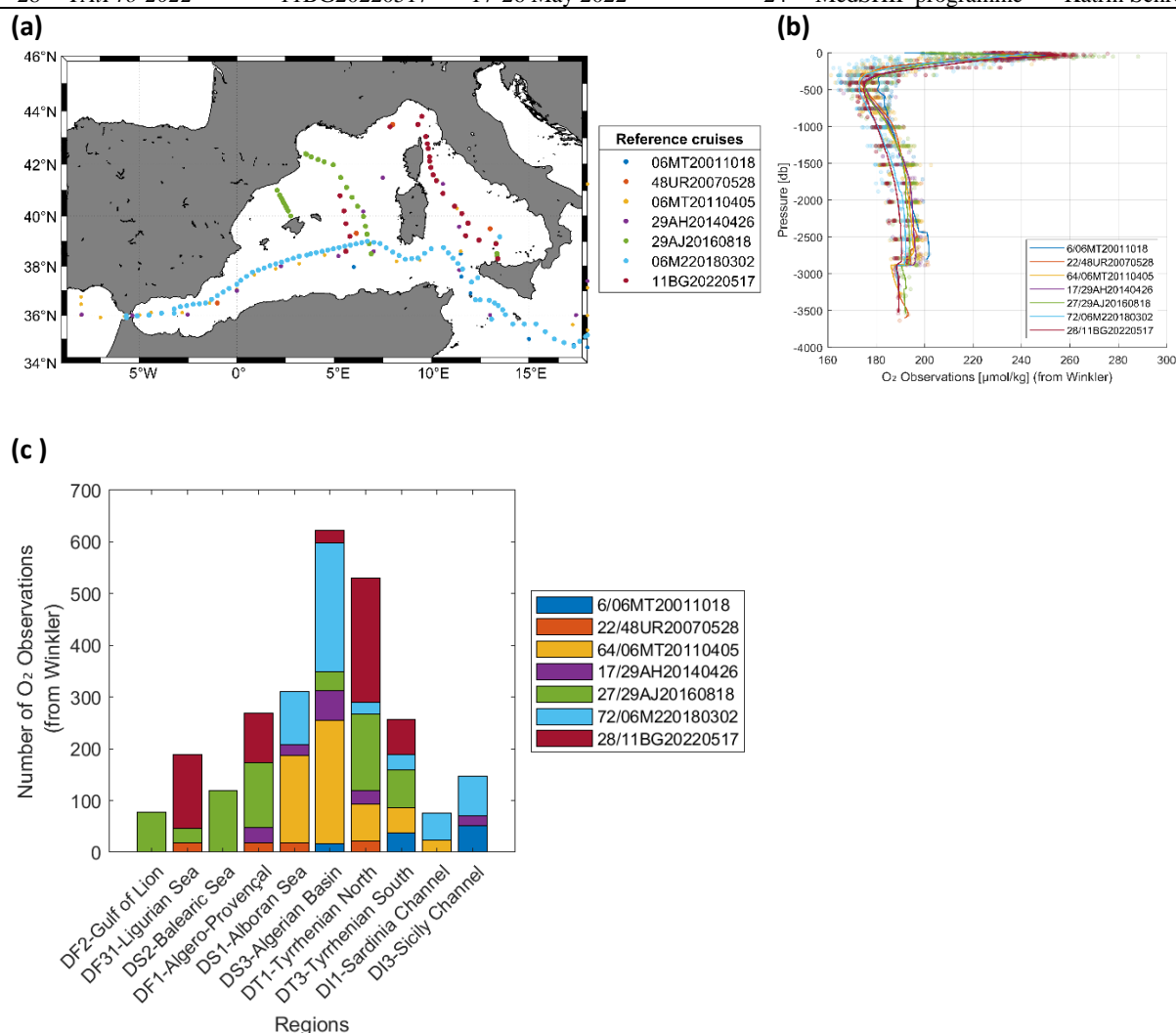


**Figure 6.** Reference cruises: (a) Map with stations. (b) Dissolved oxygen data from Winkler measurements and corresponding mean profile from the reference cruises and (c) Number of oxygen observations in the reference for each region.

Figure 6 (c) presents a histogram of the regional distribution of the reference dataset, which aligns well with CTDO2-WMED dataset. both datasets consistently highlight the Tyrrhenian (DT1) and the Algerian basin (DS3) as the most frequently sampled subregions over the multiple years.

## 281 - Accuracy envelope in the WMED

282 To explore the feasibility of applying a broader accuracy threshold specific to the WMED, we assess whether  
 283 relaxing the accuracy threshold to 2% is appropriate for the reference cruises in DS3 and DT1, two regions  
 284 representative of contrasting deep-water dynamics.

285 For this analysis, each DO profiles from selected reference were interpolated to a standard pressure grid (0 -  
 286 3600 dbar) using a piecewise cubic Hermite interpolating. Mean DO profiles were then computed per cruise  
 287 and averaged across cruises to produce a composite profile for each region (Fig.8).

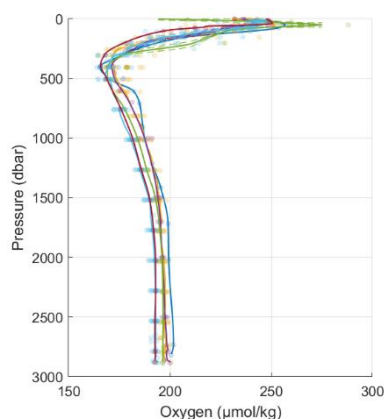
288 Both subregions display the typical WMED oxygen structure as described in section above. However, the degree  
 289 of interannual variability differs substantially between the two.

290 In the DT1 (Tyrrhenian Sea), oxygen profiles from different reference cruises show minimal variability between  
 291 800 and 2500 db, suggesting stable deep-water conditions; The Tyrrhenian deep waters are known to be ventilated  
 292 not primarily by deep convection but through lateral advection and double-diffusion process (Durante et al., 2009).  
 293 Signs of episodic ventilation, particularly in 2007 and 2016 have been identified and discussed by Li and Tanhua  
 294 (2020). The consistent/ slow increase in oxygen below 800 db likely reflect the influence of such processes, which  
 295 may also explain the weak development of a well-defined tracer minimum zone (TMZ) in this region.

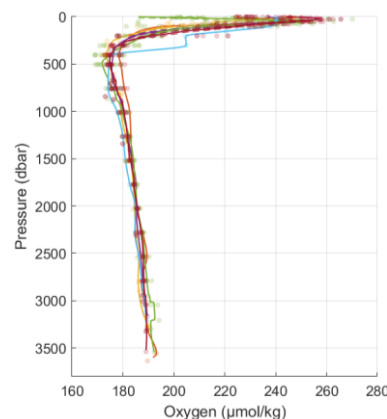
296 In contrast, DS3 (the Algerian basin) shows significantly more variability. While the overall profile shape is  
 297 consistent, DO concentrations below 1500 db in recent cruises (2018 and 2022) are lower by 4-5  $\mu\text{mol/kg}$   
 298 compared to earlier cruises. These differences correspond to deviations of 2 to 4%, likely linked to temporal  
 299 changes that may be linked shifts in deep water formation. Studies using transient tracers, have reported enhanced  
 300 ventilation between 2001 and 2016. Consistent with our observations. However, as suggested by Li & Tanhua  
 301 (2020), the declining intensity of deep convection in recent years has reduced oxygen renewal at depth, a trend  
 302 clearly evident in DS3- Algerian basin, but not observed in the DT1- Tyrrhenian Sea, as also noted by Schneider  
 303 et al. (2014)

304 Figure 7 (a,b) confirm the contrasting DO patterns between the two subregions, while , while zoomed panels (c)  
 305 and (d) highlight the spread among cruises. The greater variability in DS3 supports the need to relax the 2<sup>nd</sup> QC  
 306 threshold from 1% to 2% to accommodate natural variability rather than forcing potentially misleading corrections.

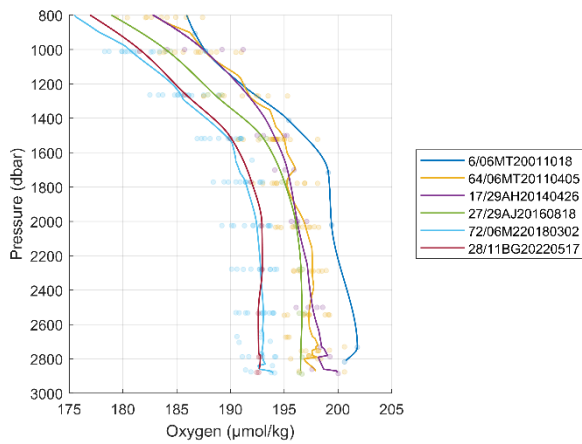
(a) DS3- Algerian basin



(b) DT1- Tyrrhenian Sea



(c)



(d)

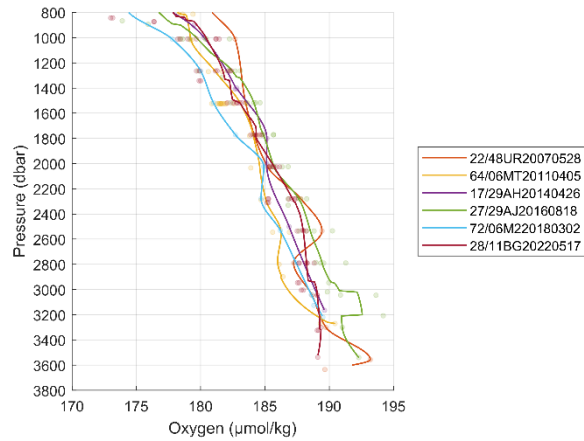


**Figure 7.** Average vertical profiles of dissolved oxygen in (a) the Algerian Basin and (b) the Tyrrhenian Sea. Panels (c) and (d) provide a zoomed view of the deep layers below 800 db. Colored dots represent individual oxygen sample, color-coded by cruise, while the solid-colored lines show the cruise-specific average profiles.

#### - Defining a stable pressure range for crossover analysis

To assess consistency in the deep layer of the reference dataset, we computed pairwise ratios (A/B) of average dissolved oxygen between the tested cruise (e.g., A:6/06MT20011018) and the six reference cruises (B). the results are shown in Figure 8 and Figure S1-2S.

In DS3 (Algerian basin), 29.7% of pairwise ratio fall within 1%, and 60.5% within 2%, while 39% exceed the 2% threshold, highlighting higher variability compared to DT1( Tyrrhenian Sea), where 71.7% of ratios lie within 1%, and 98.7% within 2%, indicating more stable deep-water conditions. Most discrepancies in both regions occur below 2500 db where data are sparser and naturel variability increases.

Cruise 72(2018) and 28 (2022) in DS3 consistently show 2-4% lower oxygen than earlier cruises (64, 17, 27), suggesting long-term decrease in oxygen or episodic variability. These patterns align with Gregoire et al.( 2023) and personal communication with L.Coppola, who attributed the 2022 anomaly to reduced deep convection. The regionally stable layer across cruises lies between 800 and 2000 db, where interannual variability is minimal. This depth range aligns with tracer minimum zone described by Li and Tanhua (2020), which reflects shifting ventilation intensity over time. Given our dataset spans 2001/ 2004-2023 , a broader 800-2000 db is proposed for crossover analysis to account for temporal and spatial changes.

This assessment follows secondary quality control procedures in the WMED; by adopting a 2% threshold, more appropriate than 1% standard used in CARINA and GLODAP; we minimize the risk of applying unjustified corrections to CTD oxygen data and accommodate the natural change in the region.



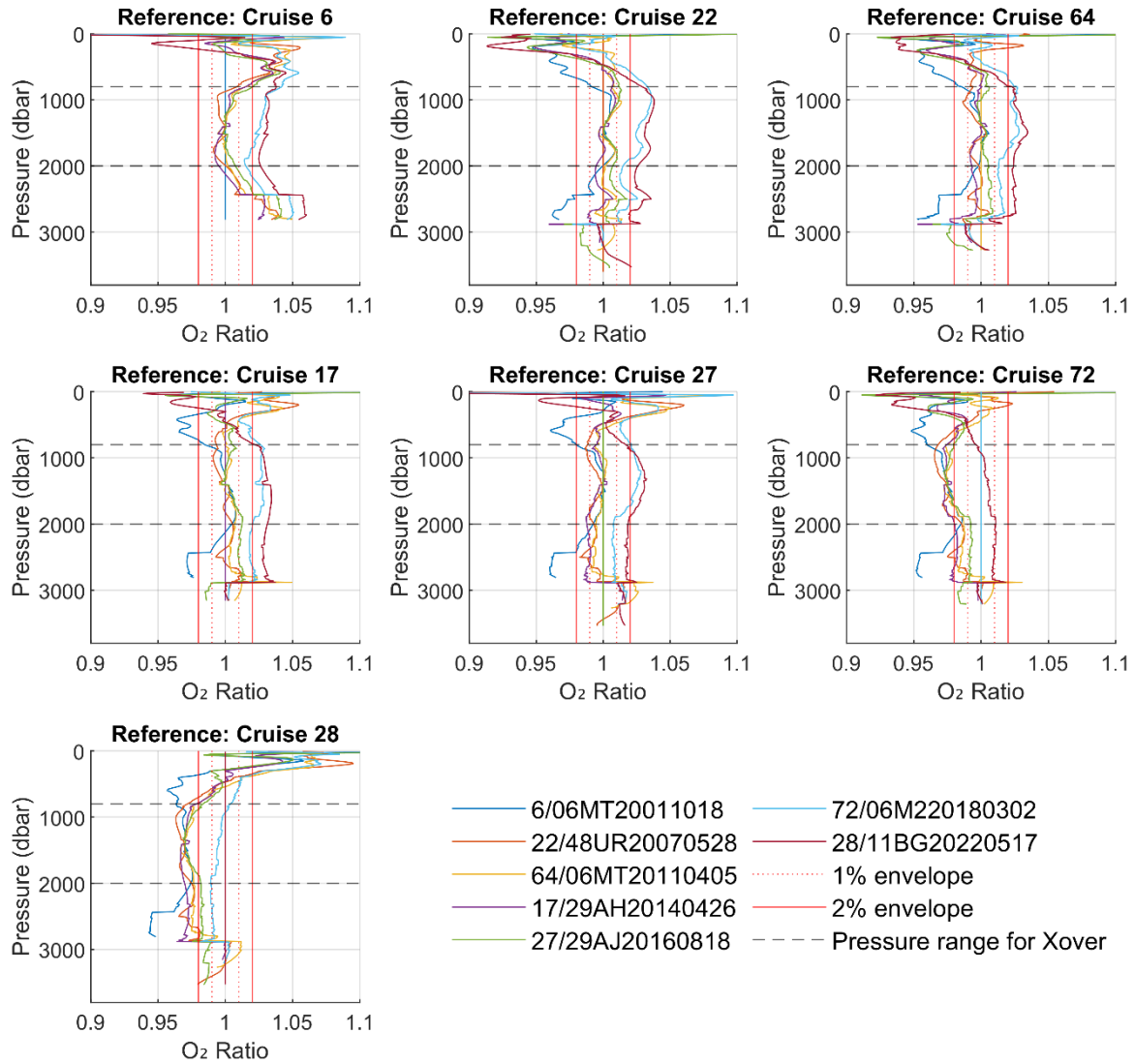


**Figure 8.** Vertical distribution of the ratio between the tested reference cruise (top of each subplot) vs the other references (in the legend box below). red continuous vertical line refer 2% accuracy envelope and red dashed line refer to 1% envelope to . Similar composite figures are in supplement for subregions DT1(Fig. S1) and DS3 (Fig. S2)(zoom: 800-2000 dbar)

- *Crossover analysis:*

A crossover analysis, following the approach of Johnson et al. (2001), Tanhua et al., (2011) and Lauvset and Tanhua (2015), was conducted. Crossover analysis (Xover) was performed by checking the cruises CTDO2-WMED dataset to the reference cruises. The method is based on the comparison of cruise pairs, where the differences between two cruises within a predefined spatial distance, here a radius of  $2^{\circ}$  latitude (approximately 222 km) are assessed. The interpolated profiles for each station in cruise C1 were compared to the interpolated profiles from cruise C2 within the specified maximum distance. A difference profile was generated for each pair of stations, with a minimum of three stations required for each crossover. Calculations were performed on density surfaces to ensure that data comparisons were made between the same or comparable water masses, thereby mitigating biases associated with variations in salinity. Density values were calculated for each measurement, and data from each profile were interpolated using a piecewise cubic Hermite interpolating scheme to standard density levels. This iterative process was repeated for each station in the cruise, resulting in multiple difference profiles.

The outcome is the weighted mean and standard deviation of the difference profiles for each cruise, referred to as the offset. The weighting applied to the profiles is based on their variability, giving higher importance to parts of the profiles with lower variability (adapted from Tanhua et al. 2010, 2015). In addition to conducting crossover analysis over the full spatial extent of each cruise, regional crossovers also performed using a modified clustering approach. In this method, clusters are manually defined based on predefined geographical subregions (Table S2); When sufficient profile coverage was available, analysis was focused on the most frequently sampled areas: the Tyrrhenian Sea (both DT1 & DT3), Algerian basin (DS3 & DF1) and the Alboran sea (DS1), as previously described. This regionalized approach helps reduce the likelihood of comparing stations influenced by distinct hydrographic regimes.

Figure 9 illustrates an example of a crossover and offset between cruise pairs over the entire region, while an overview of some crossovers vs. reference dataset are displayed in Section 4. All calculated offsets for each cruise were examined to determine the presence of any likely biases in the measurements.

The number of stations in the overlapping region (i.e., within the predefined radius) is critical for accurate offset estimation. For instance, as depicted in Figure 8 (a), 30 stations from C1 were compared to 14 stations from C2 to estimate the offset; a limited number of stations can introduce uncertainty into the offset estimate. Additionally, while the number of crossover cruises is significant, the Mediterranean Sea has a limited number of reference cruises available.

Corrections Factor (CF) is estimated from the offset. CF were meticulously reviewed and justified whenever adjustments were deemed necessary (Table 4), at this step, a set of potential correction factor is estimated from the difference offsets. Here, we followed a conservative approach, we are comparing the median regional offsets and choose to apply the correction factor with an absolute low percent of change (deviation from 1). This approach is ensuring low change in the data and improves the internal consistency of the data.

Following adjustments/corrections, the last step involves evaluation the overall internal consistency of the entire dataset CTDO2-WMED using the weighted mean (WM) of the absolute offsets ( $D$ ) of all crossovers ( $L$ ) and the standard deviation ( $\sigma$ ), following Tanhua et al. (2009) and Belgacem et al. (2020). This assessment quantifies the accuracy of the data product, as supported by previous studies (Hoppema et al., 2009; Sabine et al., 2010; Tanhua et al., 2009). Notably, our evaluation is based on offsets relative to a reference dataset, providing a comprehensive understanding of data consistency.

$$WM = \frac{\sum_{i=1}^L D(i) / (\sigma(i))^2}{\sum_{i=1}^L 1 / (\sigma(i))^2}$$

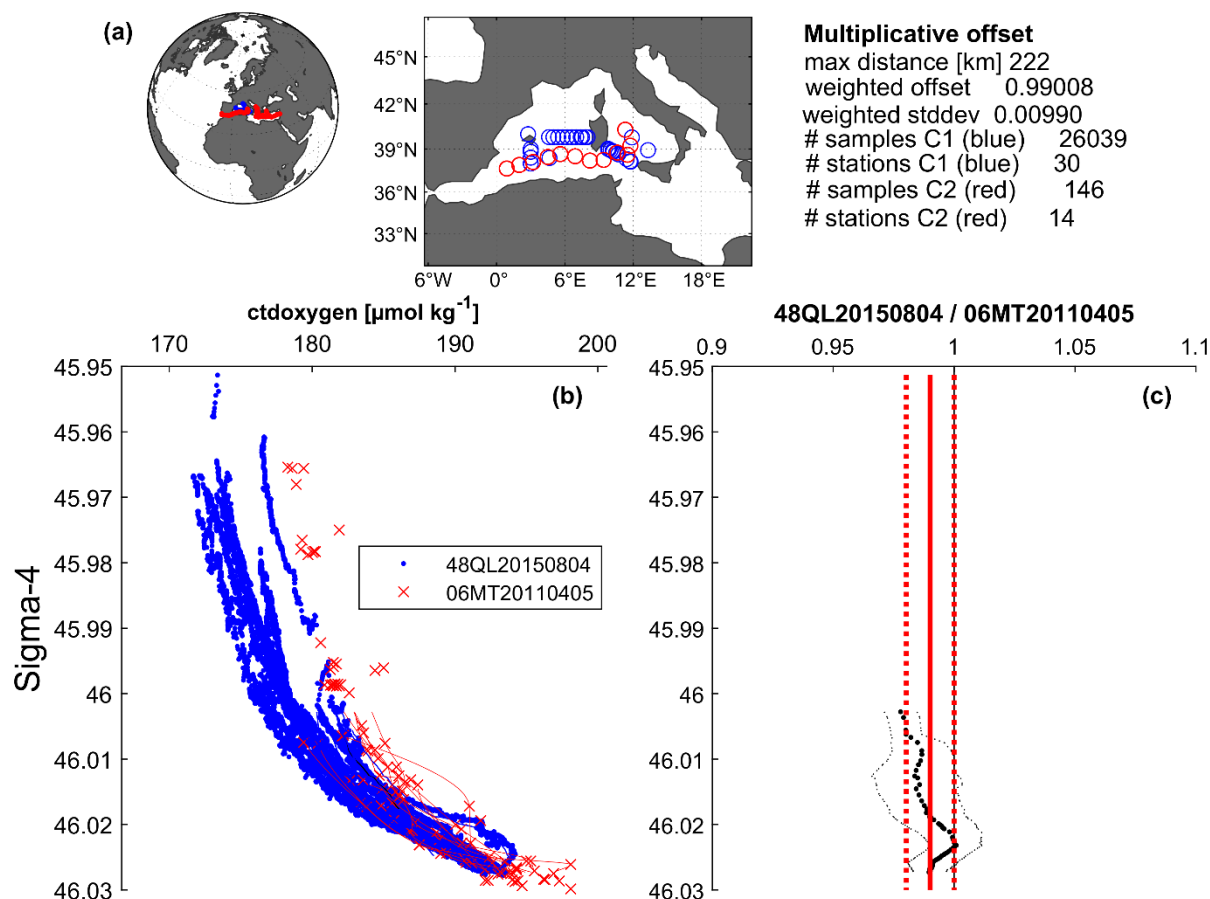


**Figure 9.** An illustration showcasing the calculated offset for dissolved oxygen between cruise 48QL20150804 and cruise 06MT20110405 (reference cruise). (a) Spatial distribution of CTD stations involved in the crossover analysis, along with statistical information. (b) Vertical profiles of dissolved oxygen observation ( $\mu\text{mol/kg}$ ) from both cruises that fall within the radius of  $2^\circ$  (800- 2500 dbar). (c) Display of the difference between both cruises (thick dotted black line), standard deviation (thin dotted black lines), the weighted average of the offset (solid red line), and the weighted standard deviation (dotted red line).

#### 4 Results of the secondary QC and recommendations

The outcomes of the crossover analysis are presented in terms of correction factors derived from comparisons with selected reference cruises (Table 2). These corrections, aimed at enhancing measurement consistency, are summarized in Table 4. The analysis assumes that the reference dataset represents the true values. This section details the various crossovers, discusses the offsets, and outlines the derived correction factors. Each crossover was thoroughly evaluated, and corrections were refined as necessary, considering the number of crossovers, regional difference and the stations involved in each comparison.

The offsets and correction factors for each cruise indicated small changes. Few cruises fell outside the predefined accuracy envelope of 2% and therefore required adjustments. Notably, cruises no. 25: 48DP20180918, no. 27: 48DP20221015, and no. 28: 48DP20230324 were excluded from the crossover analysis due to an insufficient number of stations below 800 dbar; however, these cruises remain available in the final dataset.

In total, 265 crossovers were identified (including the entire extent and regional clustering) of the cruises and the regional . The analysis suggested that deep oxygen measurements from specific cruises (no. 2, no.8, no.211 and no.222) necessitated upward adjustment when compared to the reference cruises in the region. Conversely, cruises

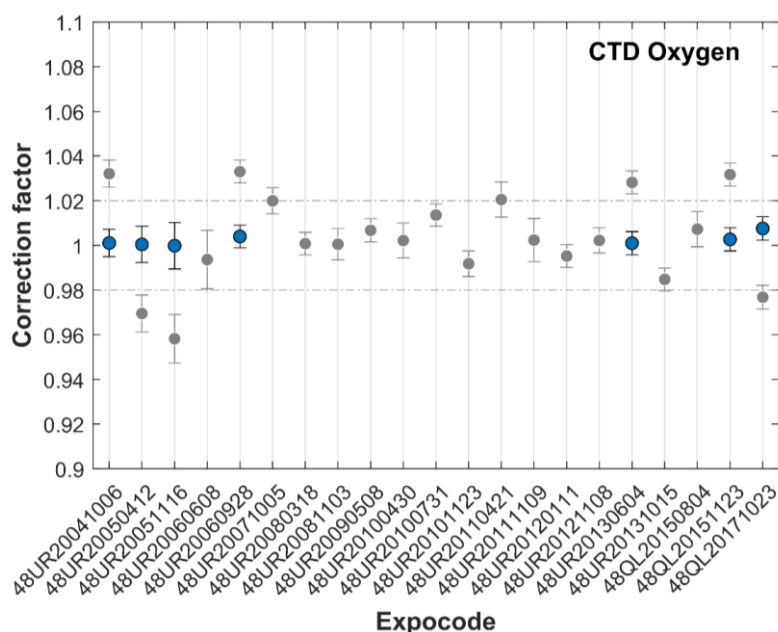
no. 3, no. 5, and no. 24 exhibited slightly elevated values relative to the respective reference datasets, indicating a need for downward adjustments. Fourteen cruises did not require any corrections, demonstrating consistency with the reference dataset and indicating a high quality of the measurements. A correction is endorsed when the offset is outside the predefined accuracy envelope of  $\pm 2\%$ .

Table 3 and Figure 10, resume the possible improvements after corrections. In the subsequent text, a thorough discussion about the adjustments (i.e., Correction factor) of the main challenging cruises is provided. The reader is invited to compare the descriptions with the respective plots in Figure 10 and the corresponding crossover summary figures for each cruise.

To validate our findings, we recalculated the offsets using the adjusted data after applying the corrections outlined in Table 4.

Following the application of these adjustments, the offsets were reduced. The suggested cruises now fall within the accepted envelope of 2% indicating an enhanced consistency of the measurements. This improvement is evident in the adjusted data presented in Figure 10(in blue).

To evaluate the consistency, we computed WM using the offsets of the crossover estimated the selected adjusted data, Figure 11. The level of internal consistency of the adjusted CTD oxygen dataset is estimated to 0.998. The adjustments removed potential biases arising from errors related to measurement, calibration, data handling practices, and the lack of adherence to international standards improving the overall consistency.



**Figure 10.** Results of the crossover analysis results for CTD dissolved oxygen, showing the recommended correction before (in grey) and after (in blue) adjustment. Error bars indicate the standard deviation of the absolute weighted offset. A correction means the original CTD Oxygen data must be multiplied by that amount (see Table 4). The dashed line represents the 2% accuracy envelope for an adjustment to be made.

**Table 3.** Summary of the suggested multiplicative adjustments for CTD dissolved oxygen resulting from the 2nd quality control

Cruise ID	EXPOCODE	Recommended correction (x)
2	48UR20041006	1.032
3	48UR20050412	0.97
5	48UR20051116	0.96
6	48UR20060608	-
8	48UR20060928	1.03
9	48UR20071005	-
10	48UR20080318	-
11/12 <sup>a</sup>	48UR20080905/48UR20081103	-
13	48UR20090508	-
14	48UR20100430	-
15	48UR20100731	-
16	48UR20101123	-
17	48UR20110421	-
18	48UR20111109	-
20	48UR20120111	-
21	48UR20121108	-
211	48UR20130604	1.028
22	48UR20131015	-
222	48QL20151123	1.03
23	48QL20150804	-
24	48QL20171023	0.97

<sup>a</sup> Cruise #11 and cruise #12 were merged in the 2<sup>nd</sup> QC.

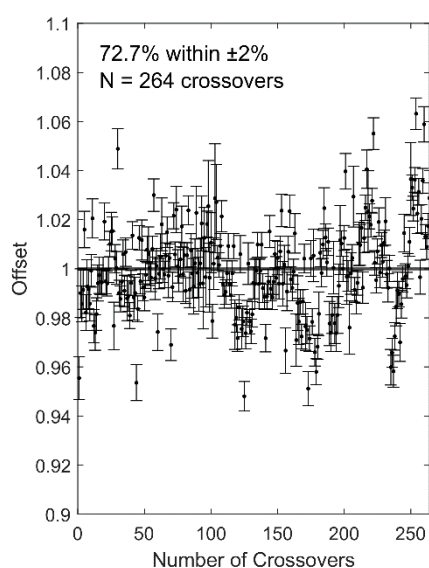


**Figure 11.** offsets calculated from CTD oxygen crossovers in CTDO2-WMED dataset after applying correction factors. N is number of crossovers.

- *CTD-O<sub>2</sub> adjustments*

In section, we provide interpretations and recommendations supporting the proposed adjustments, including discussion of any potential offsets identified, even for cruise where no correction was ultimately applied. Cruises not mentioned here showed consistent CTD oxygen data and required no further review. All applied corrections are summarized in Table 3.

**Cruise no. 2 (48UR20041006)** has crossovers in three sub-regions: two in the Alboran sea, five and four in the Algerian basin and the Tyrrhenian. Offsets in the three regions demonstrated a consensus regarding a mean offset of 0.96 to 0.96 (Fig. 12).

agree about the increase and data of cruise 48UR20041006 seems to be lower than the reference cruises by 4%. In Figure 3, the mean residual between Winkler and Sensor was higher than 2  $\mu\text{mol/kg}$ , which might indicate calibration issue. While this increase may appear excessive, it is important to consider that the regional deep averages obtained from cruise no.2 were the lowest (Fig. 5). Adding to this, the WMED deep layer before 2004, has stable ventilation, it is after 2004 the decline in ventilation has been noted. This may provide a rational for the adjustment. That is to say that cruise 48UR20041006 could not have lower. We are applying in all regions the lowest correction factor that changes in a minimum way the data among the different regions which is an increase of 3.2% that means a correction factor of 1.032.

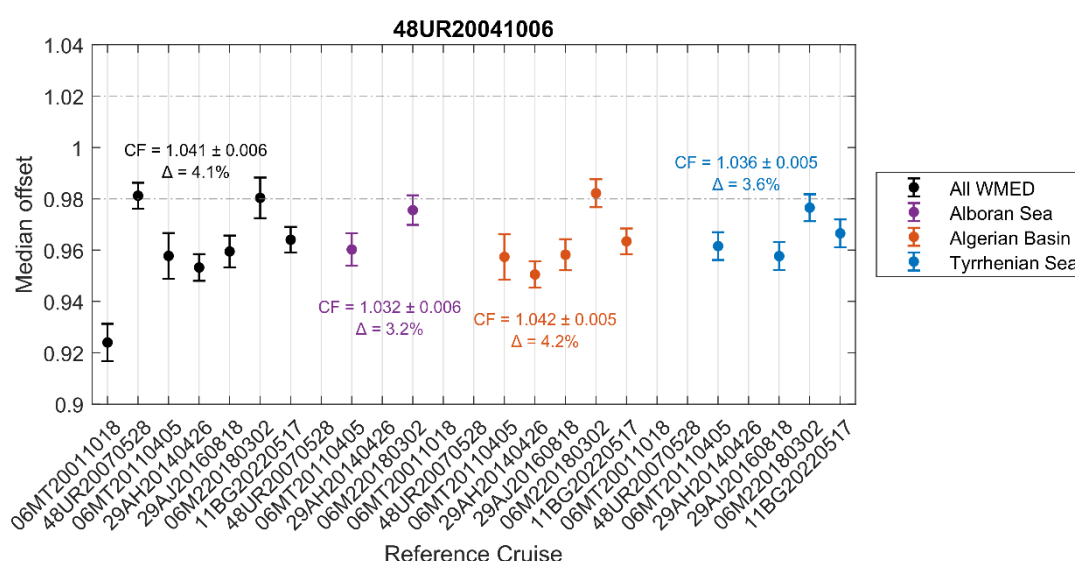


**Figure 12.** Summary of offsets for all crossovers found for CTD oxygen on cruise no. 2/48UR20041006. The solid red line indicates the weighted mean of the offsets, with its standard deviation in dashed lines; the dashed grey lines denote the predefined accuracy limits for Oxygen measurements; the black dots with error bars illustrate the weighted median offsets in relation to individual reference cruises, along with their corresponding weighted standard deviations in all WMED, the purple is for the Alboran Sea, Orange for the Algerian basin and blue for the Tyrrhenian. The correction factor, standard deviation, and percentage of change of these offsets in each subregion are annotated within the figure. Note that the reference cruises along the x-axis are arranged in chronological order for the different subregions.

Data from cruise **no.3 48UR20050412** was compared to the same reference cruises as cruise no.2. The offset between cruise no.3 and the reference cruises in the Algerian basin with five crossovers and four crossovers in the Tyrrhenian Sea indicates that an adjustment toward a decrease is necessary. As pointed out in section 3.1 cruise no.3 could be of low precision compared to cruises conducted in the same regions.

Based on the agreement between the offsets in both the two subregions (Fig. 13), and even though the crossover with reference 2001 showed good agreement (based on 3station in 3different geographic areas), it does not seem robust. So, for this cruise, the offset we are using the overall offset of 1.03 (all WMED), that suggests correction factor of 0.97 which supports a downward adjustment of  $\sim 3\%$ .



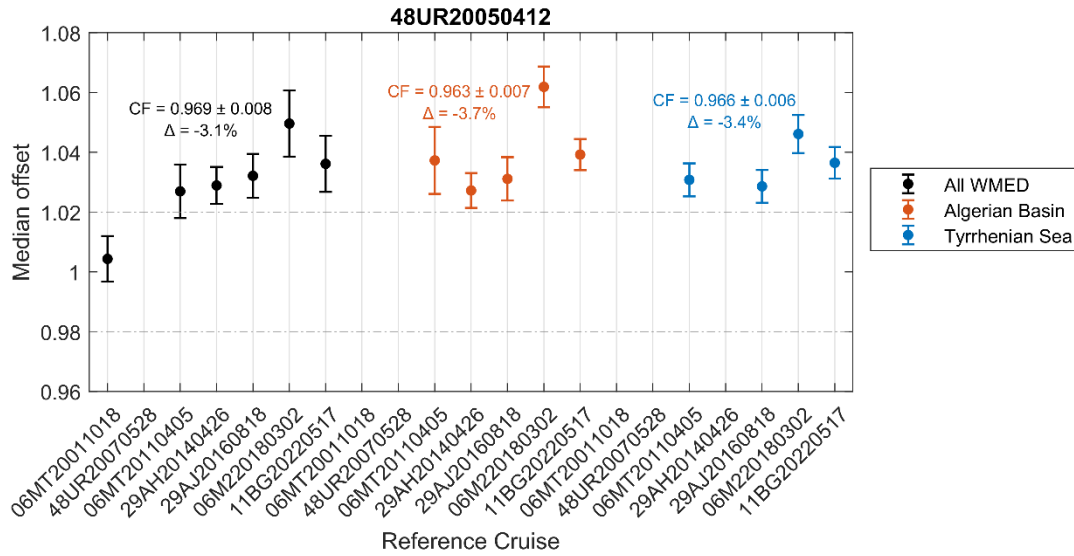


**Figure 13.** The same as Fig.12 but for cruise no.3 48UR20050412

Cruise **no. 5 (48UR20051116)** had four crossovers in the Tyrrhenian Sea spanning the years 2011, 2016, 2018 and 2022 (Fig.S3). there is a good agreement in terms of in the precision shown in the weighted standard deviation of 0.01. A median of the weighted offset of 1.042 is found. Based on this, an adjustment toward a decrease of ~4.2% is suggested for cruise no.5. The discrepancy may indicate potential issues with sensor. An adjustment of 0.96 is suggested.

**Cruise no. 6 (48UR20060608)** has five crossovers in the Algerian basin and four in the Tyrrhenian Sea (Fig. 14). Offsets in the overall basin and in the Algerian basin showed an increased trend of the offset with time. Seven crossovers out of 9 from both subregions were within the 2% envelope.

Here the dynamic between both subregion is clear, low weighted standard deviation of 0.005 in the Tyrrhenian indicate the good precision and good agreement between the four crossovers. In area the variability is less pronounced. While in the Algerian known to be highly variable area, and very much representing the direct effect of the Gulf on Lion, had larger standard deviation of 0.01 persistent in all with references except the 2022 reference.

We refrained from adjusting the data because most of the crossovers did not show consistency between regions and potential trends is observed similar to average vertical profile in Fig.7(c) of the reference cruises in the Algerian and there was good agreement with the references. The majority of the crossover fall within the 2% accuracy. No adjustment is needed.

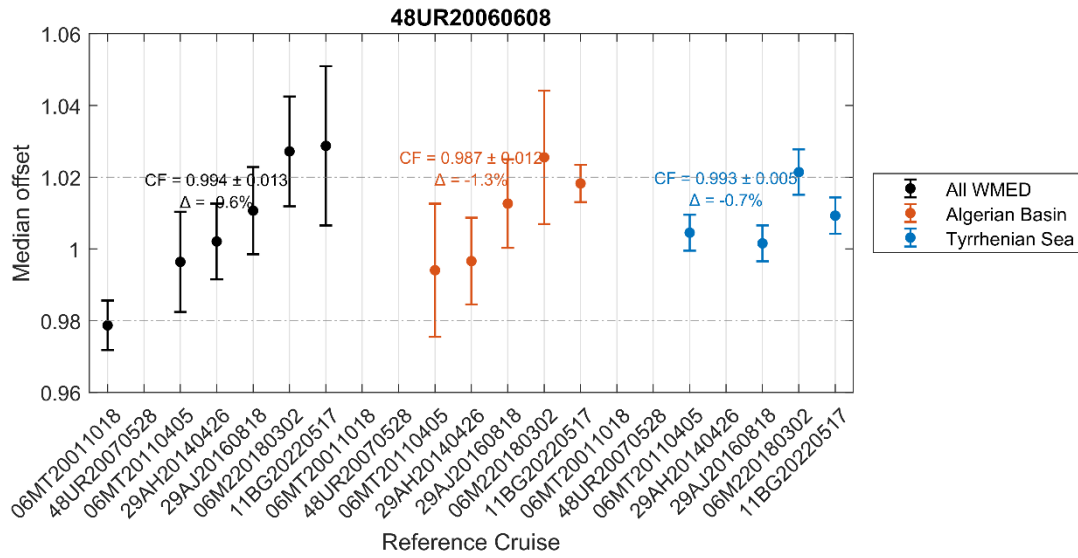


**Figure 14.** The same as Fig.12 but for Cruise no. 6 (48UR20060608).

**Cruise no. 8 (48UR20060928)** four crossovers in the Tyrrhenian Sea with reference cruises 06MT20110405, 29AJ20160818, 06M220180302 and 11BG20220517, they all agree about the 0.005 standard deviation and the good quality of the data (Fig. S4). All offsets vary between 0.96 and 0.97 pointing to a correction toward an increase of ~3%. The offsets are outside the 2% envelope. Here we suggest an adjustment of 1.03.

**Cruise no. 9 (48UR20071005)** has five crossovers in the Algerian basin and four crossovers in the Tyrrhenian Sea. All showing median standard deviation of 0.005 indicative of the good precision of the data. Median weighted offset of 0.97 is recorded in the Tyrrhenian and 0.98 in the Algerian basin. The largest offset was with 06MT20011018, where the offset is about 0.95 (Fig. 15), likely due to the large scatter among the limited number of stations in both sub-regions. Despite, both subregions show a consistent deviation of about the 2% increase, thus suggesting a correction factor of 1.02 that is within the 2% envelope. Therefore, no correction is recommended for this cruise.

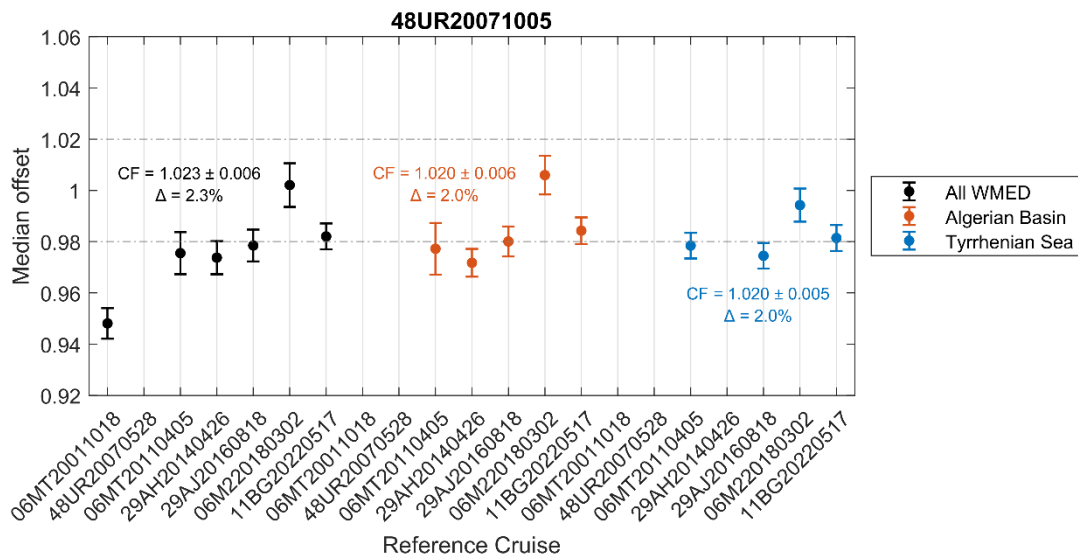
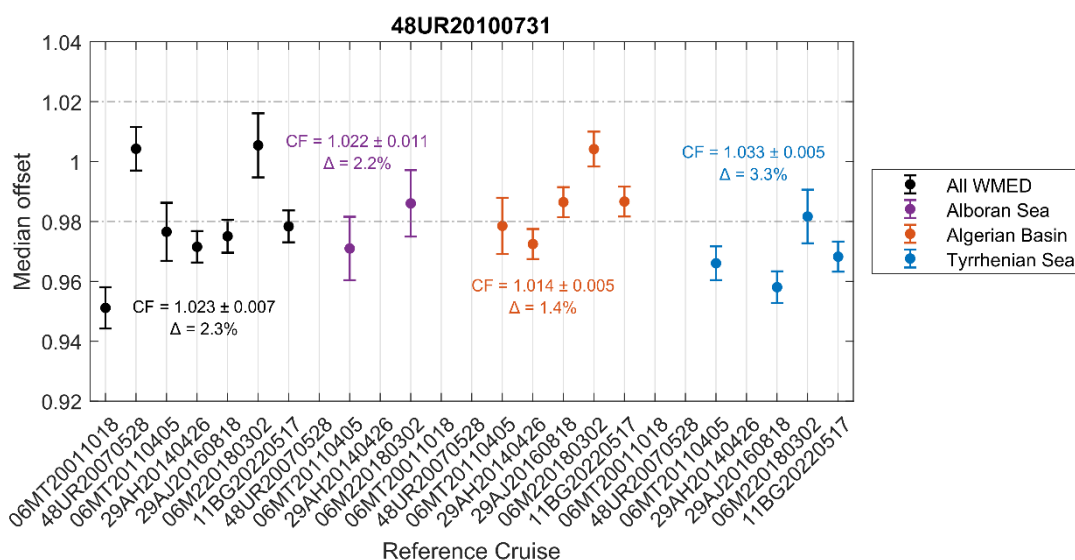


**Figure 15.** The same as Fig.12 but for Cruise no. 9 (48UR20071005).

494

495 **Cruise no. 15 (48UR20100731)** has two crossovers in the Alboran Sea with a median offset of  $0.98 \pm 0.01$ , five  
 496 crossovers in the Algerian basin with an offset of  $0.98 \pm 0.005$ , and four crossovers in the Tyrrhenian Sea showing  
 497 an offset of  $0.97 \pm 0.005$  (Fig.16). The data appear to be of good quality overall. Following our conservative  
 498 correction approach, the lowest observed percentage of change is 1.4, suggesting a correction factor of 1.014, that  
 499 is well within the  $\pm 2\%$  acceptance envelope. Therefore, no adjustment is applied.



500

501 **Figure 16.** The same as Fig.12 but for Cruise no. 15 (48UR20100731).

502 **Cruise no. 211 (48UR20130604)** has an offset of 6% increase in oxygen observed the Algerian basin. A lower  
 503 offset magnitude is noted in the Tyrrhenian proposing an increase of 2.8%. Both median offsets indicate that  
 504 oxygen data for this cruise are lower than the references, although data precision appears good. In contrast, cruise  
 505 **no. 22 (48UR20131015)** from the same year shows smaller offsets magnitude in both regions (Fig.S5), suggesting  
 506 its oxygen values are higher than the references and might require a small downward adjustment. However, the  
 507 proposed correction factor  $0.98 \pm 0.005$  for cruise no.22 remain within the 2 % envelope, so no adjustment is  
 508 applied. For cruise no.211, the differing offset magnitudes between the Algerian and Tyrrhenian (6% vs. 2.8%,  
 509 respectively, Fig. 17) present a discrepancy; to balance these regional differences while respecting the predefined  
 510  $\pm 2\%$  envelope, we recommend applying a correction factor of 1.028. this value reflects the smaller offset found  
 511 in the Tyrrhenian Sea and avoids overcorrecting the data, ensuring consistency.

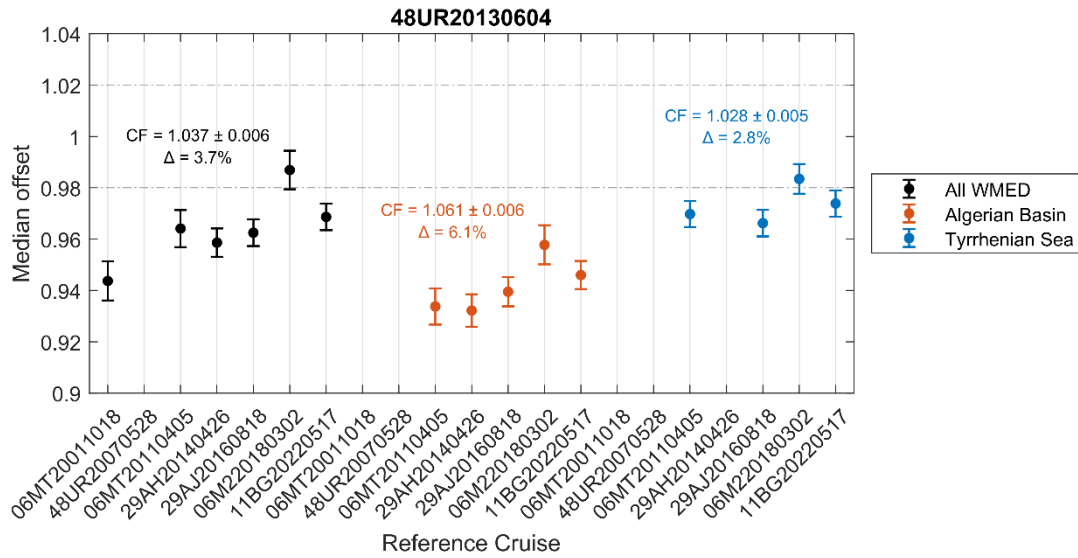


**Figure 17.** The same as Fig.12 but for Cruise no. 211 (48UR20130604).

**Cruise no. 222 (48QL20151123)** show a consistent median offset of 0.97 across four crossovers in the Tyrrhenian Sea, spanning multiple years (Fig. S6). The data exhibit good precision, with a weighted standard deviation of 0.005. however, the persistent offset magnitude indicates a systematic underestimation of the oxygen relative to the reference. Deep measurement from this cruise seems to be lower than the reference suggesting a correction of 3% toward an increase, corresponding to a correction factor of 1.03.

**Cruise no. 24 (48QL20171023)** has four crossovers over the Tyrrhenian Sea (Fig. S7) and shows CTD oxygen values were slightly higher than the reference cruises. The median offset suggests a decrease of approximately 2.3%, indicating a correction factor of 0.97. precision remain high with, weighted standard deviation of 0.005. Additionally, as shown in Figure 3, the means residuals between Winkler and sensor measurements for this cruise was classified as poor, further supporting the need for adjustment. We decided to apply the correction.

## 5 Summary and conclusions

This study aimed to evaluate and enhance the consistency and accuracy of CTD oxygen measurements in the WMED by implementing the 2nd QC procedure based on crossover analysis. Recognizing the limitations of applying a uniform 1% accuracy envelope; originally developed for the Atlantic datasets; we identified a more regionally appropriate threshold of  $\pm 2\%$  for the deep Mediterranean layers, particularly within 800-2000 db range. This adjustment better reflects the natural variability and ventilation dynamics specific to the region.

As part of the 2<sup>nd</sup> QC of the CTDO<sub>2</sub>-WMED dataset, a total of 265 crossover comparison were conducted, both spatially and regionally, using a set of high-quality reference cruises. The methodology presented here provides a robust framework for future quality control efforts in regions with similarly complex hydrographic conditions. While the majority of cruises fell within the revised  $\pm 2\%$  envelope, a few showed systematic offsets that warranted correction. Adjustments were applied conservatively, only when deviations exceeded the defined threshold and considering the lowest percentage of change; and are recommended for seven cruises. Although the quality of these cruises is considerate moderate, they remain valuable for long-term trend analyses Rather than being flagged, they are included in the final product. These adjustments led to measurable improvements in data consistency,

increasing the internal agreement across cruises, as evidenced by the weighted mean of 0.998. Although a few cruises lacked sufficient deep profiles to perform crossover analysis, their data are retained in the final dataset. Importantly, the dataset aligns with FAIR data principles, and openly accessible.

Despite limitations in temporal coverage and the finite number of reference cruises, this updated dataset significantly enhances our understanding of long-term dissolved oxygen variability in the WMED. It complements and extends earlier efforts in the region (Schneider et al., 2014; Coppola and al. (2017); Moriarty et al., 2017; Macías et al., 2018b; Mavropoulou et al., 2020 ;Li & Tanhua (2020); Cossarini et al., 2021; Friedland et al., 2021 ;Ulses and al. (2021), and Fourrier et al. (2022).

Dissolved oxygen is a robust tracer for assessing both physical and biogeochemical changes, carrying the imprint of water mass since their last ventilation. As global warming increases ocean stratification (Oschlies et al., 2008), vertical mixing and thus oxygen renewal is expected to decline, contributing to long-term deoxygenation. This trend is further amplified by increasing ocean heat content and acidification in surface layer (Yao et al., 2016; Reale et al., 2021).

Given the scarcity of high-resolution oxygen observations in space and time, recent advances using model simulations, machine learning, and autonomous platforms such as BGC-Argo floats and gliders are crucial. The CTDO2-WMED dataset, in combination with these emerging sources, provides a valuable foundation for assessing changes in the oxygen budget of the Mediterranean Sea. it supports ongoing efforts to understand the region's response to climate -driven oceanographic changes and to improve future projections.

## 6 Data availability

The CNR\_O2WMEDv1 (Belgacem et al., 2024 [in review], see temporary link below) dataset is available at PANGAEA (submitted on 21/08/2024, DOI in preparation). It consists of two parts; the first an aggregation of the cruises prior correction which has undergone both calibration and 1<sup>st</sup> quality check. The second is the adjusted data product using the recommended corrections from the secondary quality control. The dataset is complementary to the data product CNR-DIN-WMED available <https://doi.org/10.1594/PANGAEA.904172>. No special software is required to access the data. the data from the reference cruises are not included in the final product. Table 6 summarizes the list of parameters included.

**Table 4. Summary of data product parameters and units.**

Variable	Data Product file parameter name	Data product WOCE flag name	Units
Expedition/cruise code	EXPOCODE		
Cruise ID	CRUISE		
Station number	STNNBR		
Year	YEAR		
Month	MONTH		
Day	DAY		
Latitude	LATITUDE		decimal degree
Longitude	LONGITUDE		decimal degree
Pressure	CTDPRS		decibar
Temperature	CTDTMP		°C
Salinity	CTDSAL	CTDSAL_FLAG_W	
Oxygen	CTDOXY	CTDOXY_FLAG_W	μmol kg <sup>-1</sup>

## Authors contributions

MaB ran the analysis and wrote the manuscript. KS contributed to writing the manuscript. MA, SKL contributed to the analysis. JC contributed to specific parts of the manuscript. MiB and SS coordinated the technical aspects of most of the cruises. CC and TC assisted some of the chemical analysis.

## Competing interest

The authors declare that they have no conflict of interest.

## Acknowledgements

M. Belgacem was supported by the EuroGO-SHIP project funded by European Union under grant agreement no. 101094690. The data have been collected in the framework of several national and European projects, e.g. KM3NeT, EU GA no. 011937; SESAME, EU GA no. GOCE-036949; PERSEUS, EU GA no. 287600; OCEAN-CERTAIN, EU GA no. 603773; COMMON SENSE, EU GA no. 228344; EUROFLEETS, EU GA no. 228344; EUROFLEETS2, EU GA no. 312762; JERICO, EU GA no. 262584; and the Italian PRIN 2007 program “Tyrrhenian Seamounts ecosystems” and the Italian RITMARE flagship project, both funded by the Italian Ministry of Education, University and Research. We acknowledge PRIN-CLOSER “CLimate forcing On Adriatic SEa deoxygenation: A multi-archive Reconstruction of Saproel S1 (CLOSER)” project funded by the Italian Ministry of Education and European Union NextGenerationEU. The authors are deeply indebted to all investigators and analysts who contributed to data collection at sea during so many years as well as to the PIs of the cruises (Stefano Cozzi, Gabriella Cerrati, Stefano Aliani, Mario Astraldi, Maurizio Azzaro, Alberto Ribotti, Massimiliano Dibitetto, Gian Pietro Gasparini, Annalisa Griffa, Jeff Haun, Loïc Jullion, Gina La Spada, Elena Mannini, Angelo Perilli and Chiara Santinelli), the captains, and the crews for allowing the collection of this enormous dataset; without them, this work would not have been possible.



## 595    **References**

- 596    Álvarez, M., Sanleón-Bartolomé, H., Tanhua, T., Mintrop, L., Luchetta, A., Cantoni, C., Schroeder, K., and  
597    Civitarese, G.: The CO<sub>2</sub> system in the Mediterranean Sea: a basin wide perspective, *Ocean Sci.*, 10, 69–92,  
598    <https://doi.org/10.5194/os-10-69-2014>, 2014.
- 599    Álvarez, M., Catalá, T. S., Civitarese, G., Coppola, L., Hassoun, A. E. R., Ibello, V., Lazzari, P., Lefevre, D.,  
600    Marcias, D., Santinelli, C., and Ulses, C: Chapter 11–Mediterranean Sea general biogeochemistry, Editor (s):  
601    Katrin Schroeder, Jacopo Chiggiato, *Oceanography of the Mediterranean Sea*, [https://doi.org/10.1016/B978-0-12-](https://doi.org/10.1016/B978-0-12-823692-5.00004-2)  
602    [823692-5.00004-2](https://doi.org/10.1016/B978-0-12-823692-5.00004-2), 2022.
- 603    Belgacem, M., Chiggiato, J., Borghini, M., Pavoni, B., Cerrati, G., Acri, F; Cozzi, S., Ribotti, A., Álvarez, M.,  
604    Lauvset, S. K., and Schroeder, K.: Quality controlled dataset of dissolved inorganic nutrients in the western  
605    Mediterranean Sea (2004– 2017) from R/V oceanographic cruises, PANGAEA [data set],  
606    <https://doi.org/10.1594/PANGAEA.904172>, 2019.
- 607    Belgacem, M., Chiggiato, J., Borghini, M., Pavoni, B., Cerrati, G., Acri, F., Cozzi, S., Ribotti, A., Álvarez, M.,  
608    Lauvset, S. K., and Schroeder, K.: Dissolved inorganic nutrients in the western Mediterranean Sea (2004–2017),  
609    *Earth Syst. Sci. Data*, 12, 1985–2011, <https://doi.org/10.5194/essd-12-1985-2020>, 2020.
- 610    Belgacem, M., Schroeder, K., Lauvset, S. K., Álvarez, M., Chiggiato, J., Borghini, M., Cantoni, C., Ciuffardi, T.,  
611    Sparnocchia, S.: O2WMED: Quality controlled dataset of dissolved oxygen in the western Mediterranean Sea  
612    (2004–2023) from R/V oceanographic cruises [dataset], PANGAEA, in review: temporary link: [https://cnrsc-](https://cnrsc-my.sharepoint.com/:f/g/personal/malekbelgacem_cnr_it/EkIgo958UMlBmJ8SGwNB4HwBBX-FzDa8NI9C3vHeS4Vd4Q?e=Wt8pII)  
613    [my.sharepoint.com/:f/g/personal/malekbelgacem\\_cnr\\_it/EkIgo958UMlBmJ8SGwNB4HwBBX-](https://cnrsc-my.sharepoint.com/:f/g/personal/malekbelgacem_cnr_it/EkIgo958UMlBmJ8SGwNB4HwBBX-FzDa8NI9C3vHeS4Vd4Q?e=Wt8pII)  
614    [FzDa8NI9C3vHeS4Vd4Q?e=Wt8pII](https://cnrsc-my.sharepoint.com/:f/g/personal/malekbelgacem_cnr_it/EkIgo958UMlBmJ8SGwNB4HwBBX-FzDa8NI9C3vHeS4Vd4Q?e=Wt8pII), 2024.
- 615    Coppola, L., Prieur, L., Taupier-Letage, I., Estournel, C., Testor, P., Lefevre, D., Belamari, S., & Taillandier, V.:  
616    Observation of oxygen ventilation into deep waters through targeted deployment of multiple Argo-O<sub>2</sub> floats in the  
617    north-western Mediterranean Sea in 2013, *J. Geophys. Res.-Oceans*, 122, 6325–6341,  
618    <https://doi.org/10.1002/2016JC012594>, 2017.
- 619    Coppola, L., Legendre, L., Lefevre, D., Prieur, L., Taillandier, V., & Riquier, E. D. (2018). Seasonal and inter-  
620    annual variations of dissolved oxygen in the northwestern Mediterranean Sea (DYFAMED site). *Progress in*  
621    *Oceanography*, 162, 187–201, <https://doi.org/10.1016/j.pocean.2018.03.001>, 2018.
- 622    Cossarini, G., Feudale, L., Teruzzi, A., Bolzon, G., Coidessa, G., Solidoro, C., Di Biagio, V., Amadio, C., Lazzari,  
623    P., Brosich, A., and Salon, S.: High-resolution reanalysis of the Mediterranean Sea biogeochemistry (1999–2019),  
624    *Front. Mar. Sci.*, 8, 741486, <https://doi.org/10.3389/fmars.2021.741486>, 2021.
- 625    Fichaut, M., Garcia, M. J., Giorgetti, A., Iona, A., Kuznetsov, A., Rixen, M., and Medar Group:  
626    MEDAR/MEDATLAS 2002: A Mediterranean and Black Sea database for operational oceanography, Elsevier  
627    *Oceanography Series*, 69, 645–648, [https://doi.org/10.1016/S0422-9894\(03\)80107-1](https://doi.org/10.1016/S0422-9894(03)80107-1), 2003.
- 628    Fourier, M., Coppola, L., Lebrato, M., Testor, P., Bosse, A., D'Ortenzio, F., Taillandier, V., de Madron, X. D.,  
629    Mortier, L., Prieur, L., and Gatti, J.: Impact of intermittent convection in the northwestern Mediterranean Sea on  
630    oxygen content, nutrients, and the carbonate system, *J. Geophys. Res.-Oceans*, 127, e2022JC018615,  
631    <https://doi.org/10.1029/2022JC018615>, 2022.
- 632    Friedland, R., Macias, D., Cossarini, G., Daewel, U., Estournel, C., Garcia-Gorriz, E., Grizzetti, B., Grégoire, M.,  
633    Gustafson, B., Kalaroni, S., Kerimoglu, O., Lazzari, P., Lenhart, H., Lessin, G., Maljutenko, I., Miladinova, S.,  
634    Müller-Karulis, B., Neumann, T., Parn, O., Pätsch, J., Piroddi, C., Raudsepp, U., Schrum, C., Stegert, C., Stips,  
635    A., Tsiaras, K., Ulses, C., and Vandenbulcke, L.: Effects of nutrient management scenarios on marine  
636    eutrophication indicators: a pan-European, multi-model assessment in support of the Marine Strategy Framework  
637    Directive, *Front. Mar. Sci.*, 8, 596126, <https://doi.org/10.3389/fmars.2021.596126>, 2021.
- 638    Garcia and Gordon (1992) "Oxygen solubility in seawater: Better fitting equations", *Limnology & Oceanography*,  
639    vol 37(6), p1307-1312.

640 Grasshoff, K., Ehrhardt, M., and Kremling, K.: Methods of Seawater Analysis, 2nd Edition, Verlag Chemie  
641 Weinheim, New York, 419 p., 1983.

642 Grasshoff, K., Kremling, K., and Ehrhardt, M.: Methods of seawater analysis (3rd edn.), Weinheim Press, WILEY-  
643 VCH, 203–273, 1999.

644 Grégoire, M., Oschlies, A., Canfield, D., Castro, C., Ciglenc̆ki, I., Croot, P., Salin, K., Schneider, B., Serret, P.,  
645 Slomp, C.P., Tesi, T., Yücel, M. (2023). Ocean Oxygen: the role of the Ocean in the oxygen we breathe and the  
646 threat of deoxygenation. Rodriguez Perez, A., Kellett, P., Alexander, B., Muñiz Piniella, Á., Van Elslander, J.,  
647 Heymans, J. J., [Eds.] Future Science Brief No. 10 of the European Marine Board, Ostend, Belgium. ISSN: 2593-  
648 5232. ISBN: 9789464206180. DOI: 10.5281/zenodo.7941157, 2023.

649 Guy, S.-V., Kress, N., Silverman, J., Gertner, Y., Ozer, T., Biton, E., Lazar, A., Gertman, I., Rahav, E., and Herut,  
650 B.: Post-eastern Mediterranean Transient Oxygen Decline in the Deep Waters of the Southeast Mediterranean Sea  
651 Supports Weakening of Ventilation Rates, *Front. Mar. Sci.*, 7, <https://doi.org/10.3389/FMARS.2020.598686>,  
652 2021.

653 Hainbucher, D., Rubino, A., Cardin, V., Tanhua, T., Schroeder, K., and Bensi, M.: Hydrographic situation during  
654 cruise M84/3 and P414 (spring 2011) in the Mediterranean Sea, *Ocean Sci.*, 10, 669–682,  
655 <https://doi.org/10.5194/os-10-669-2014>, 2014.

656 Helen, R., Powley., Krom, M. D., Van Cappellen, P.: Circulation and oxygen cycling in the Mediterranean Sea:  
657 Sensitivity to future climate change, *J. Geophys. Res.*, <https://doi.org/10.1002/2016JC012224>, 2016.

658 Hoppema, M., Velo, A., van Heuven, S., Tanhua, T., Key, R. M., Lin, X., Bakker, D. C. E., Perez, F. F., Ríos, A.  
659 F., Lo Monaco, C., Sabine, C. L., Álvarez, M., and Bellerby, R. G. J.: Consistency of cruise data of the CARINA  
660 database in the Atlantic sector of the Southern Ocean, *Earth Syst. Sci. Data*, 1, 63–75, <https://doi.org/10.5194/essd-1-63-2009>, 2009.

662 Janzen, C., Murphy, D., and Larson, N.: Getting more mileage out of dissolved oxygen sensors in long-term  
663 moored applications, *OCEANS 2007, IEEE*, doi: 10.1109/OCEANS.2007.4449398, 2007.

664 Johnson, G. C., Robbins, P. E., and Hufford, G. E.: Systematic adjustments of hydrographic sections for internal  
665 consistency, *J. Atmos. Ocean. Tech.*, 18, 1234–1244, [https://doi.org/10.1175/1520-0426\(2001\)018<1234:SAOHSF>2.0.CO;2](https://doi.org/10.1175/1520-0426(2001)018<1234:SAOHSF>2.0.CO;2), 2001.

667 Jullion, L.: TALPro2016: A Tyrrhenian Sea & Alger-Provençal component of the MedSHIP Programme, RV  
668 Angeles Alvarino, 18/08/16 – 29/08/16, Palermo (Italy) – Barcelona (Spain), Bremerhaven, EUROFLEETS2  
669 Cruise Summary Report, <https://epic.awi.de/id/eprint/49725/>, 2016.

670 Keeling, R. F., Körtzinger, A., and Gruber, N.: Ocean deoxygenation in a warming world, *Annu. Rev. Mar. Sci.*,  
671 2, 199–229, doi: 10.1146/annurev.marine.010908.163855, 2010.

672 Langdon, C.: Determination of Dissolved Oxygen in Seawater by Winkler Titration using Amperometric  
673 Technique, In: Hood, E.M., Sabine, C.L., Sloyan, B.M. (Eds.), *The GO-SHIP Repeat Hydrography Manual: A*  
674 *Collection of Expert Reports and Guidelines, Version 1*, IOCCP Report Number 14, ICPO Publication Series  
675 Number 134, 18pp., <https://doi.org/10.25607/OBP-1350>, 2010.

676 Lauvset, S. K., and Tanhua, T.: A toolbox for secondary quality control on ocean chemistry and hydrographic data,  
677 *Limnol. Oceanogr. Methods*, 13, 601–608, <https://doi.org/10.1002/lom3.10050>, 2015.

678 Li P and Tanhua T (2020) Recent Changes in Deep Ventilation of the Mediterranean Sea; Evidence From Long-  
679 Term Transient Tracer Observations. *Front. Mar. Sci.* 7:594. doi: 10.3389/fmars.2020.00594

680 Liu G., Yu,X., Zhang,J., Wang,X., Xu,N., Ali,S.: Reconstruction of the three-dimensional dissolved oxygen and  
681 its spatio-temporal variations in the Mediterranean Sea using machine learning, *Journal of Environmental*  
682 *Sciences*,2025,ISSN 1001-0742,<https://doi.org/10.1016/j.jes.2025.01.010>.

683 Manca, B., Burca, M., Giorgetti, A., Coatanoan, C., Garcia, M. J., and Iona, A. Physical and biochemical averaged  
684 vertical profiles in the Mediterranean regions: an important tool to trace the climatology of water masses and to  
685 validate incoming data from operational oceanography, *J. Mar. Syst.*, 48, 83–116,  
686 <https://doi.org/10.1016/j.jmarsys.2003.11.025>, 2004.

687 Macias, D., Garcia-Gorrioz, E., and Stips, A.: Deep winter convection and phytoplankton dynamics in the NW  
688 Mediterranean Sea under present climate and future (horizon 2030) scenarios, *Sci. Rep.*, 8, 6626,  
689 <https://doi.org/10.1038/s41598-018-24978-5>, 2018.

690 Margirier, F., Testor, P., Heslop, E., Mallil, K., Bosse, A., Houpert, L., Mortier, L., Bouin, M.-N., Coppola, L.,  
691 D’Ortenzio, F., Durrieu de Madron, X., Mourre, B., Prieur, L., Raimbault, P., and Taillandier, V.: Abrupt warming  
692 and salinification of intermediate waters interplays with decline of deep convection in the Northwestern  
693 Mediterranean Sea, *Sci. Rep.*, 10, 20923, <https://doi.org/10.1038/s41598-020-77961-9>, 2020.

694 Martínez, J., Leonelli, F. E., García-Ladona, E., Garrabou, J., Kersting, D. K., Bensoussan, N., and Pisano, A.:  
695 Evolution of marine heatwaves in warming seas: the Mediterranean Sea case study, *Front. Mar. Sci.*, 10, 1193164,  
696 <https://doi.org/10.3389/fmars.2023.1193164>, 2023.

697 Marullo, S., De Toma, V., di Sarra, A., Iacono, R., Landolfi, A., Leonelli, F., Napolitano, E., Meloni, D., Organelli,  
698 E., Pisano, A., Santoleri, R., and Sferlazzo, D.: Has the frequency of Mediterranean Marine Heatwaves really  
699 increased in the last decades? , *EGU General Assembly 2023*, Vienna, Austria, 23–28 Apr 2023, EGU23-4429,  
700 <https://doi.org/10.5194/egusphere-egu23-4429> , 2023.

701 Mavropoulou, A.-M., Vervatis, V., and Sofianos, S.: Dissolved oxygen variability in the Mediterranean Sea, *J.*  
702 *Mar. Syst.*, 208, 103348, <https://doi.org/10.1016/j.jmarsys.2020.103348> ,2020.

703 Mavropoulou, A.-M.: Mediterranean Sea: Dissolved Oxygen, Temperature and Salinity Annual Variability and  
704 Monthly Climatology for the period 1960-2011, <https://doi.org/10.5281/zenodo.3878076> , 2020.

705 Middleton, L., Wu, W., Johnston, T. M. S., Tarry, D. R., Farrar, J. T., Poulain, P.-M., Özgökmen, T. M.,  
706 Shcherbina, A. Y., Pascual, A., McNeill, C. L., Belgacem, M., Berta, M., Abbott, K., Worden, A. Z., Wittmers,  
707 F., Kinsella, A., Centurioni, L. R., Hormann, V., Cutolo, E., Tintoré, J., Ruiz, S., Casas, B., Cheslack, H.,  
708 CALYPSO Collaboration, D’Asaro, E. A., and Mahadevan, A.: Ocean cyclone splitting ventilates the upper ocean,  
709 *Sci. Adv.*, accepted, 2025.

710 Moriarty, J. M., Harris, C. K., Fennel, K., Friedrichs, M. A. M., Xu, K., and Rabouille, C.: The roles of  
711 resuspension, diffusion and biogeochemical processes on oxygen dynamics offshore of the Rhône River, France:  
712 a numerical modeling study, *Biogeosciences*, 14, 1919–1946, <https://doi.org/10.5194/bg-14-1919-2017>, 2017.

713 Olsen, A., Key, R. M., van Heuven, S., Lauvset, S. K., Velo, A., Lin, X., Schirnick, C., Kozyr, A., Tanhua, T.,  
714 Hoppema, M., Jutterström, S., Steinfeldt, R., Jeansson, E., Ishii, M., Pérez, F. F., and Suzuki, T.: The Global Ocean  
715 Data Analysis Project version 2 (GLODAPv2) – an internally consistent data product for the world ocean, *Earth*  
716 *Syst. Sci. Data*, 8, 297–323, <https://doi.org/10.5194/essd-8-297-2016> , 2016.

717 Olsen, A., Lange, N., Key, R. M., Tanhua, T., Bittig, H. C., Kozyr, A., Álvarez, M., Azetsu-Scott, K., Becker, S.,  
718 Brown, P. J., Carter, B. R., Cotrim da Cunha, L., Feely, R. A., van Heuven, S., Hoppema, M., Ishii, M., Jeansson,  
719 E., Jutterström, S., Landa, C. S., Lauvset, S. K., Michaelis, P., Murata, A., Pérez, F. F., Pfeil, B., Schirnick, C.,  
720 Steinfeldt, R., Suzuki, T., Tilbrook, B., Velo, A., Wanninkhof, R., and Woosley, R. J.: An updated version of the  
721 global interior ocean biogeochemical data product, GLODAPv2.2020, *Earth Syst. Sci. Data*, 12, 3653–3678,  
722 <https://doi.org/10.5194/essd-12-3653-2020> , 2020.

723 Owens, W. B., and R. C. Millard Jr., 1985: A new algorithm for CTD oxygen calibration. *J. Physical*  
724 *Oceanography*, 15, 621-631.

725 Pastor, F., and Khodayar, S.: Marine heat waves: Characterizing a major climate impact in the Mediterranean,  
 726 EGU General Assembly 2023, Vienna, Austria, 24–28 Apr 2023, EGU23-13058,  
 727 <https://doi.org/10.5194/egusphere-egu23-13058>, 2023.

728 Reale, M., Cossarini, G., Lazzari, P., Lovato, T., Bolzon, G., Masina, S., Solidoro, C., and Salon, S.: Acidification,  
 729 deoxygenation, and nutrient and biomass declines in a warming Mediterranean Sea, *Biogeosciences*, 19, 4035–  
 730 4065, <https://doi.org/10.5194/bg-19-4035-2022>, 2022.

731 Ribotti, A., Sorgente, R., Pessini, F., Cucco, A., Quattrocchi, G., and Borghini, M.: Twenty-one years of  
 732 hydrological data acquisition in the Mediterranean Sea: quality, availability, and research, *Earth Syst. Sci. Data*,  
 733 14, 4187–4199, <https://doi.org/10.5194/essd-14-4187-2022>, 2022.

734 Schroeder, K., Tanhua, T., Bryden, H., Alvarez, M., Chiggiato, J., and Aracri, S.: Mediterranean Sea Ship-based  
 735 Hydrographic Investigations Program (Med-SHIP), *Oceanography*, 28, 12–15,  
 736 <https://doi.org/10.5670/oceanog.2015.71>, 2015.

737 Schneider, A., Tanhua, T., Roether, W., and Steinfeldt, R.: Changes in ventilation of the Mediterranean Sea during  
 738 the past 25 year, *Ocean Sci.*, 10, 1–16, <https://doi.org/10.5194/os-10-1-2014>, 2014.

739 Schroeder, K., Kovačević, V., Civitarese, G., Velaoras, D., Álvarez, M., Tanhua, T., Jullio, L., Coppola, L., Bensi,  
 740 M., Ursella, L., Santinelli, C., Giani, M., Chiggiato, J., Aly-Eldeen, M., Assimakopoulou, G., Bachi, G., Bogner,  
 741 B., Borghini, M., Cardin, V., Cornec, M., Giannakourou, A., Giannoudi, L., Gogou, A., Golbol, M., Or Hazan, O.,  
 742 Karthäuser, C., Kralj, M., Krasakopoulou, E., Matić, F., Mihanović, H., Muslim, S., Papadopoulos, V.P., Parinos,  
 743 C., Paulitschke, A., Pavlidou, A., Pitta, E., Protopapa, M., Rahav, E., Raveh, O., Renieris, P., Reyes-Suarez, N.  
 744 C., Rousselaki, E., Silverman, J., Souvermezoglou, E., Urbini, L., Zer, C., and Zervoudaki, S.: Seawater physics  
 745 and chemistry along the Med-SHIP transects in the Mediterranean Sea in 2016, *Sci. Data*, 11, 52,  
 746 <https://doi.org/10.1038/s41597-023-02835-3>, 2024.

747 Schroeder, K.: TALPro2022 CRUISE REPORT R/V BELGICA Cruise n. 2022/12 (Version 1), Zenodo,  
 748 <https://doi.org/10.5281/zenodo.6918731>, 2022.

749 Tanhua, T., Brown, P. J., and Key, R. M.: CARINA: nutrient data in the Atlantic Ocean, *Earth Syst. Sci. Data*, 1,  
 750 7–24, <https://doi.org/10.5194/essd-1-7-2009>, 2009.

751 Tanhua, T.: Matlab Toolbox to Perform Secondary Quality Control (2nd QC) on Hydrographic Data, ORNL  
 752 CDIAC-158, Carbon Dioxide Inf. Anal. Center, Oak Ridge Natl. Lab., U.S. Dep. Energy, Oak Ridge, Tennessee,  
 753 158, <https://doi.org/10.1002/lom3.10050>, 2010.

754 Tanhua, T.: Hydrochemistry of water samples during MedSHIP cruise Talpro, PANGAEA,  
 755 <https://doi.org/10.1594/PANGAEA.902293>, 2019a.

756 Tanhua, T.: Physical oceanography during MedSHIP cruise Talpro [dataset], PANGAEA,  
 757 <https://doi.org/10.1594/PANGAEA.902330>, 2019b.

758 Testor, P., Bosse, A., Houpert, L., Margirier, F., Mortier, L., Legoff, H., Dausse, D., Labaste, M., Bouin, M.-N.,  
 759 Coppola, L., Koenig, Z., Damien, P., et al.: Multiscale observations of deep convection in the northwestern  
 760 Mediterranean Sea during winter 2012–2013 using multiple platforms, *J. Geophys. Res.-Oceans*, 122, 1745–1776,  
 761 <https://doi.org/10.1002/2016JC012671>, 2017.

762 Uchida, H. Johnson, G. C. and McTaggart, G. C.: CTD Oxygen Sensor Calibration Procedures. In, The GO-SHIP  
 763 Repeat Hydrography Manual: A Collection of Expert Reports and Guidelines. Version 1, (eds Hood, E.M., C.L.  
 764 Sabine, and B.M. Sloyan), 17pp. (IOCCP Report Number 14; ICPO Publication Series Number 134),  
 765 <https://doi.org/10.25607/OBP-1344>, 2010.

766 Ulses, C., D'Ortenzio, F., Coppola, L., Estournel, C., Testor, P., Marsaleix, P., Prieur, L., Taillandier, V., Dumas,  
 767 F., Severin, T., and Conan, P.: Oxygen budget of the north-western Mediterranean deep-convection region,  
 768 *Biogeosciences*, 18, 937–960, <https://doi.org/10.5194/bg-18-937-2021>, 2021.

769 Yao, M., Marcou, O., Goyet, C., Guglielmi, V., Touratier, F., and Savy, J.-P.: Time variability of the north-western  
770 Mediterranean Sea pH over 1995–2011, *Mar. Environ. Res.*, 116, 51–60,  
771 <https://doi.org/10.1016/j.marenvres.2016.02.016>, 2016.